Impact of acidity and surface modulated acid dissociation on cloud response to organic aerosol

Gargi Sengupta[a], Minjie Zheng[a, b], and Nønne L. Prisle[a*]

[a]Center for Atmospheric Research, University of Oulu, P.O. Box 4500, 90014 Oulu, Finland
[b]Current affiliation: Institute for Atmospheric and Climate Science, ETH Zurich, Zürich, Switzerland

Correspondence: Nønne L. Prisle (Nonne.Prisle@oulu.fi)

Abstract.

~~Dissociation of organic acids is currently not included~~ Acid dissociation of the organic aerosol fraction has the potential to impact cloud activating properties by altering aqueous phase H^+ concentrations and water activity, but is currently overlooked in most atmospheric aerosol models. ~~Organic dissociation in aqueous aerosols could alter the concentrations and affect the cloud activating properties.~~ We implemented a simple representation of organic ~~dissociation in a box model version of the aerosol–chemistry–climate model ECHAM-HAMMOZ~~ acid dissociation in the aerosol-chemistry-climate box model ECHAM6.3-HAM2.3 and investigated the impact ~~on~~ on aerosol forming aqueous Sulfur chemistry, cloud droplet number concentrations, and short-wave radiative effect~~through changes in kinetically driven sulfate concentrations in an aerosol population. Organic dissociation has been observed in X-ray photo-electron spectroscopy measurements~~ . Many atmospheric organic acids are also surface active and may be strongly adsorbed at the surface of small aqueous droplets. The degree of dissociation has recently been observed for several atmospheric surface-active organics with Brönsted acid character to be significantly ~~suppressed in the aqueous surface. We therefore additionally~~ shifted in the surface, compared to the bulk aqueous solution. In addition to the well known bulk acidity, we therefore introduced an empirical account of this ~~mechanism to~~ surface modulated dissociation to further explore the potential ~~further~~ impact on aerosol ~~effects.~~ climate effects. Malonic acid and ~~decanoic~~ Decanoic acid were used as proxies for atmospheric organic ~~acid aerosols~~ aerosols of different surface-active and acid strengths. Both acids were found to yield sufficient ~~hydrogen~~ Hydrogen ion concentrations from dissociation in an aqueous droplet population to strongly influence ~~the sulfur~~ aqueous aerosol Sulfur chemistry, leading to enhanced cloud droplet number concentrations and a cooling short-wave radiative effect. Further considering ~~surface modulated suppressed~~ the surface modulation of organic acid dissociation, the impact on cloud microphysics was smaller than according to the ~~well-known bulk solution organic dissociation~~well known bulk solution acidity, but still significant. Our results show that organic aerosol ~~acidity~~ acid dissociation can significantly influence predictions of aerosol and cloud droplet formation and aerosol-cloud-climate effects ~~. Furthermore,~~ and that, even for a well known bulk solution phenomenon such as acidity, it may be important to also consider the specific influence of surface effects ~~, also in relation to bulk solution phenomena such as organic acid dissociation~~when surface-active acids comprise a significant fraction of the total organic aerosol mass.

1 Introduction

Atmospheric aerosols are an important contributor to Earth's climate. They may either absorb or reflect heat and sunlight, directly affecting Earth's energy budget ~~(IPCC et al., 2007)~~(Stocker et al., 2014; Masson-Delmotte et al., 2021). Aerosols also contribute to the global climate through indirect effects where they serve as the necessary seeds for cloud formation (Twomey, 1977; Lohma . The chemical composition of aerosols is complex and includes numerous organic and inorganic species (O'Dowd et al., 2004; Putaud et al., 2010; Murphy et al., 2006). Organic compounds have been reported to comprise approximately ~~20 to 50~~20 – 50% of the total aerosol mass at mid-latitude regions (Saxena and Hildemann, 1996; Putaud et al., 2004) and much higher (approximately 90%) in tropical forests (Andreae and Crutzen, 1997; Roberts et al., 2001; Kanakidou et al., 2005). Significant amounts of organic aerosols (approximately ~~70%~~70% of the total aerosol mass) are also reported in the middle troposphere (Huebert et al., 2004). Despite their abundance and importance, the organic fraction is the least understood component of atmospheric aerosols and the uncertainty around organic aerosols and their interaction with clouds remains one of the largest overall sources of uncertainty in climate projections (IPCC, 2013; Seinfeld et al., 2016; Legg, 2021). ~~This is due, in part, to a limited representation~~ The size, chemical composition, and phase-state of organic aerosol (OA) ~~processes and properties in climate models~~ are known to directly impact its cloud droplet formation potential (Hallquist et al., 2009; McFiggans et al., 2006) and the radiative effect of clouds (Turnock et al., 2019). However, climate models often have a limited representation of OA processes and properties, such as ~~organic~~ acidity and surface activity of the organic components (Kanakidou et al., 2005; Prisle et al., 2012a; Freedman et al., 2018; Pye et al., 2020)~~.~~, which contribute to the overall uncertainty in predictions of OA and their interactions with clouds.

~~The acidity of aqueous aerosol droplets, reported in terms of~~ Organic aerosols contain a substantial fraction of species exhibiting Brönsted acid character (Jacob, 1986; Millet et al., 2015; Keene and Galloway, 1984; Chebbi and Carlier, 1996; Chen et al., 202 . The concentrations of acidic species in aqueous aerosols directly affect the aerosol pH ~~, is one of its most fundamental chemical properties, driving key chemical reactions that ultimately impact global climate in numerous ways (Ault, 2020). The aerosol acidity representation in climate models uses observationally-based proxies, which serve as a universal~~ by modifying the H^+ concentrations within the aerosol (Pye et al., 2020; Ault, 2020). This pH ~~indicator in simulations, however, these proxies do not represent the entire aerosol population accurately (Pye et al., 2020). Studies comparing different model estimates of~~ affects the dissociation of individual acidic species with significant consequences for aerosol chemistry (Hung et al., 2018; Wang et al., 2 and phase state (Liu et al., 2019). For example, pH ~~using the same inputs differ on average by 0.3 units (but can vary up to 1 unit, increasing with decreasing relative humidity) depending on the model framework used and the approach for estimating the activity coefficient (Peng et al., 2019; Ruan et al., 2022; Battaglia Jr et al., 2021). While gas-particle partitioning and ionic equilibria are the dominant factors that drive aerosol acidity, models are frequently lacking that is kinetically generated as a result of transient gas- and liquid-phase chemical reactions (Li et al., 2022; Tilgner et al., 2013). Additionally, the organic fraction, which often comprises significant amounts of components with acid functionality, is considered as un-dissociated and the concentration in aerosols is assumed to have no contribution from the organic fraction (Kanakidou et al., 2005; Hennigan et al., 2015) . The dissociation of the organic fraction in aqueous aerosols could play a significant role in the measure of aerosol acidity and~~

influence chemical processes within the aerosol, such as the oxidation of sulfur dioxide by and , leading to increased sulfate concentrations dependent Sulfur oxidation (Liu et al., 2020) and salt formation by acidic or basic OA (Yli-Juuti et al., 2013) can each lead to significant mass formation and alter the overall chemical composition of aerosols. The chemical form (protonated or deprotonated) of acidic OA and contributions to the number of solute species in the aqueous aerosols (Liu et al., 2020) . The inclusion of organic dissociation in climate models could impact fundamental aerosol chemical processes and therefore, have a significant impact on the cloud activation properties of aqueous aerosols . aerosol phase can strongly affect water activity and condensation–evaporation equilibrium (Prisle, 2006; Prisle et al., 2008; Frosch et al., 2011; Michailoudi et al., 2019).

Many atmospheric organic acids also exhibit surface activity in aqueous solutions, such as aqueous aerosols and cloud droplets (Prisle, 2023). Surface active organics (surfactants) have been reported in atmospheric aerosols from many different regions and environments (Gérard et al., 2016; Petters and Petters, 2016; Nozière et al., 2017; Kroflič et al., 2018; Gérard et al., 2019b) . In liquid mixtures, such as aqueous solution droplets, surfactants can (Gérard et al., 2016; Petters and Petters, 2016; Nozière et al., 2017; K . Surfactants adsorb at the interfaces, lowering the surface tension and inducing concentration gradients between the droplet surface and bulksolution (Prisle et al., 2010b; Bzdek et al., 2020; Lin et al., 2018; Malila and Prisle, 2018; Lin et al., 2020; Prisle, 2021) . The bulk-surface partitioning may be significant in small droplets like atmospheric aerosols due to the aqueous surface, leading to enhanced surface concentrations compared to the interior (bulk) of a solution. In microscopic and submicron-sized aerosols and droplets, the surface adsorption can result in significant redistribution of surface active OA mass from the bulk to the surface phase, so-called bulk–surface partitioning, as a consequence of the very high surface area (A) to bulk volume ratio. Therefore, surface properties should be explicitly considered to represent surface active aerosols in climate models (Prisle et al., 2010b, 2012a). (V) ratio in these size ranges (Prisle et al., 2008, 2010b). For spherical droplets of diameter $D_{\mathrm{wet}} = 0.1$, 1, and 10 µm, $A/V = 6/D_{\mathrm{wet}}$ is 60, 6, and 0.6 $\mu\mathrm{m}^{-1}$, respectively (Prisle, 2021). Thermodynamic calculations have shown that for aerosol particles containing surfactant fatty acids and their salts, organosulfates, di- and polycarboxylic acids, and complex fulvic acids, a large fraction of the surface active OA is partitioned to the surface during major parts of hygroscopic growth and cloud droplet activation (Prisle et al., 2010b, 2011; Hansen et al., 2015; Malila and Prisle, 2018; Lin et al., 2018, 2020; Prisle, 2021; Vepsä . Consequently, the chemical and physical state of the surface may significantly contribute to determining the overall aerosol properties (Prisle et al., 2012b; Bzdek et al., 2020; Prisle, 2021, 2023).

Synchrotron-radiation-based

Highly surface sensitive synchrotron radiation excited X-ray photoelectron spectroscopy (XPS) measurements in the surface region of aqueous solutions containing surface-active carboxylate ions have been used to study the acid-base speciation at the surface (Prisle et al., 2012b; Öhrwall et al., 2015b; Werner et al., 2018). These studies revealed that investigate the acid–base speciation of surface-active atmospheric Brönsted acids and bases in the surface region of aqueous solutions (Prisle et al., 2012b; Öhrwall et . In these experiments, the protonated form of the surfactant carboxylates each conjugate pair was found at an extraordinarily large fraction, compared to that expected from the bulk their acidity and the bulk solution pH. Specifically, (Werner et al., 2018) found that the surface acid-base equilibrium of Werner et al. (2018) observed a shift in the degree of protonation for simple mono-carboxylic acids was shifted by 1 – 2 at the surface in dilute aqueous solutions (50 mM Butyric and Pentanoic acid) corresponding to activating cloud droplets. The acid–base equilibrium in the surface was shifted systematically across a very

wide range of solution pH, overall corresponding to an apparent shift in pK_a on the order of $1-2$ pH units, compared to the bulk acidity across a wide range of bulk well known bulk acidity, for each of the acids. Shifts in surface protonation degree of similar magnitude were also previously observed using XPS for dilute aqueous solutions of $10-25$ mM Decanoate/Decanoic acid (Prisle et al., 2012b), 0.1 M Propanoate/Propanoic acid, and 0.1 M Octanoate/Octanoic acid (Öhrwall et al., 2015a) at near-neutral pH. XPS measurements on aqueous solutions of Succinic acid, a moderately surface-active dicarboxylic acid, over a range of concentrations from $0.05-0.5$ M and solution pH . Very few studies have investigated the consequences of varying organic acidity on cloud activation (Tilgner et al., 2021a; Angle et al., 2021; Li et al., 2020; Franco et al., 2021) and to the best of our knowledge, organic dissociation accounting for surface specific effects in aqueous aerosols has never been implemented and studied in a cloud activation model. from $2.0-12.9$ also indicated a shifted acid–base equilibrium in the surface compared to the bulk, where the protonated form showed a considerably higher propensity to reside in the aqueous surface region than its conjugate deprotonated form (Werner et al., 2014a). These observations are further supported by experiments by Wellen et al. (2017), who used surface tension titration and infrared reflection absorption spectroscopy to obtain pH dependent aqueous surface tension of Nonanoic and Decanoic acids at their aqueous solution surfaces. They inferred that the so-called surface pK_a was greater than the well known bulk pK_a by 1 pH unit for Nonanoic acid and 2 pH units for Decanoic acid, suggesting that the organic acid dissociation response to a given aqueous bulk pH is different in the surface, compared to the bulk.

The general behavior of acidic compounds at the aqueous interface is still not well constrained (Saykally, 2013). Petersen and Saykally (2 observed an enhanced surface concentration of hydronium ions in aqueous solutions of Hydroiodic acid, alkali iodides and alkali hydroxides using second harmonic generation spectroscopy experiments. This was in contrast to previous macroscopic bubble and droplet experiments, which were interpreted to indicate that hydroxide ions were enhanced at the air–water interface (Graciaa et al., 1995; Takahashi, 2005; Karraker and Radke, 2002; Creux et al., 2007). Enami et al. (2010) also made similar observations of enhanced hydronium ions in the surface of Trimethylamine solutions using electrospray mass spectrometry. Recently, Gong et al. (2023) used stimulated Raman scattering microscopy to observe enhanced concentrations of Sulfate and Bisulfate anions, with Bisulfate being more surface enriched than Sulfate, in the surface of 2.9 μm aerosol droplets generated from an aqueous solution with 300 mM $NaHSO_4$ and 50 mM Na_2SO_4 at the same pH. They interpret this as an enhancement of acidity, with approximately threefold increase in the Hydrogen ion concentration, at the droplet edge, compared to the center of the droplet. Previous observations by Margarella et al. (2013) on the dissociation of Sulfuric acid at the water interface using liquid-jet photoelectron spectroscopy, have also reported that the ratio of Bisulfate-to-Sulfate anions was higher in the surface region.

In this work, we introduce organic dissociation in the use an aerosol–chemistry-climate box model ECHAM6.3–HAM2.3 (Kokkola et al., 2018; Tegen et al., 2019), and assess its impact on sulfur chemistry and cloud activation process via cloud droplet number concentrations (CDNC) and short-wave radiative effect (RE) , as examples of key processes taking place in organic aqueous aerosols and droplets. We also implement a simple representation of surface modulated suppressed organic dissociation and investigate the significance of such an effect for predictions of aerosol–cloud–climate effects. to investigate the potential impact on aerosol forming aqueous phase Sulfur chemistry, cloud droplet activation, and aerosol-cloud-climate

parameters of organic acid dissociation in aqueous aerosols and its additional surface modulation for surfactant acidic OA. Very few studies have previously addressed the dissociation of organic components in aerosols in relation to cloud chemistry and microphysics (Tilgner et al., 2021a; Angle et al., 2021). Tilgner et al. (2021a) compiled a kinetic data set to study the implications of varying aerosol acidity on the oxidation of the protonated and deprotonated forms of atmospheric organic acids with aqueous-phase oxidants, such as OH radical, NO_3 radical, or O_3. They showed that acidity strongly affects the chemical processing of dissociating organic compounds, but did not provide a direct correlation between organic dissociation and cloud activation. Angle et al. (2021) measured the pH of nascent seaspray aerosol using a Micro-Orifice Uniform Deposit Impactor (MOUDI) and impacting the aerosols onto colorimetric pH strips. They found that the pH of freshly emitted (nascent) seaspray aerosols was approximately four pH units lower than that of sea water. The dissociation of organic acids in the aerosols is proposed as a possible factor contributing to the low nascent seaspray aerosol pH. They note that for a nascent seaspray aerosol with a diameter of 200 nm and surface layer of Palmitic acid, only 4.4% acid dissociation would be required to lower the aerosol pH from 8 to 2. However, they do not provide any details on how the organic acid dissociation would affect the aerosol properties. To the best of our knowledge, the organic acid dissociation in aqueous aerosols has never been studied in the context of a cloud activation model, let alone accounting for surface specific modulation of organic acid dissociation in aqueous aerosols.

2 Methods

We first introduce an account of ~~organic dissociation~~ well known organic acid dissociation in bulk aqueous solution and then augment it with a simple empirical representation to further ~~account for the~~ include surface-driven suppression of dissociation ~~observed in~~ according to observations from XPS measurements. ~~The impact of organic aerosol acidity and surface-driven suppressed dissociation on the sulfur chemistry and cloud microphysics is then assessed. We use ECHAM6.3~~We use ECHAM6.3–~~HAM2.3 (referred to here~~ HAM2.3 (here referred to as HAMBOX), which is a box model version of the aerosol–chemistry–climate model ECHAM–HAMMOZ (Tegen et al., 2019)~~. HAMBOX includes the SALSA2.0 sectional aerosol module as described by Kokkola et al. (2018). We calculate the~~ , to calculate the total aerosol population Sulfate mass and cloud droplet number concentrations (CDNC) for an air parcel ~~, based on the predicted total aerosol population sulfate mass accounting for the surface specific effects, and compare~~ and the short-wave radiative effect (RE) from cloud formation, as examples of key processes taking place in aqueous organic aerosols and droplets. The impact of organic aerosol bulk acidity and surface-modulated suppressed dissociation on aerosol Sulfur chemistry and cloud microphysics is assessed by comparing to predictions for identical conditions without accounting for organic acid dissociation. The ~~resulting CDNC is then used to estimate the short-wave radiative effect (RE) from cloud formation using the method of Bzdek et al. (2020).~~ simulation time for all calculations was 1 hour, with 1 second time steps.

2.1 Aerosol module in HAMBOX

HAMBOX uses the ~~SALSA2.0~~ SALSA2.0 aerosol module (Kokkola et al., 2018)~~. In SALSA2.0,~~ , where the aerosol size distribution is calculated using the sectional approach (Jacobson, 2005) and represented using ~~10~~ 10 size bins i. Here, we group the ~~10~~ 10 size bins into four sub-ranges: Nucleation (i = ~~1 and 2~~1 and 2) with mean particle diameter, $\bar{d}_p$ = ~~56~~ 56 nm; Aitken (i = ~~3, 4 and 5~~3, 4 and 5) with $\bar{d}_p$ = ~~160~~ 160 nm; Accumulation (i = ~~6, 7 and 8~~6, 7 and 8) with $\bar{d}_p$ = ~~485~~ 485 nm, and Coarse (i = ~~9 and 10~~9 and 10) with $\bar{d}_p$ = ~~1.85~~ 1.85 µm. The initial number concentration in each sub-range ~~is shown in Table 1~~(Table 1) used for all HAMBOX simulations is representative of clean environments, such as European villages (Tunved et al., 2005, 2008). As a property of the sectional approach, when particles grow or shrink out of the boundaries of their size bins, they are redistributed to new size bins and the new aerosol size distribution is calculated at each simulation time step.

Table 1. Initial aerosol number concentration in each size sub-range used in ~~HAMBOX–SALSA2.0 model~~HAMBOX–SALSA2.0, representative of clean environments Tunved et al. (2005, 2008).

Sub-range	Number concentration [~~N/cm^3~~] N cm^{-3}]	Geometric mean diameter [µm] & Standard deviation
Nucleation	~~100~~ 100	~~0.01 & 1.50~~ 0.01 & 1.50
Aitken	~~400~~ 400	~~0.3 & 1.50~~0.3 & 1.50
Accumulation	~~200~~ 200	~~1.0 & 1.50~~1.0 & 1.50
Coarse	~~0~~ 0	~~3.0 & 2.0~~ 3.0 & 2.0

A ~~sulfur~~ Sulfur chemistry module (Feichter et al., 1996a) is coupled to the aerosol growth module in ~~SALSA2.0 through time step. The sulfur~~ SALSA2.0. At each time step, the Sulfur chemistry module feeds ~~in the calculated sulfate~~ the calculated Sulfate mass fraction in the aerosol population ~~to~~ into the growth module, ~~the growth module~~ which undergoes an aerosol redistribution and feeds back the new aerosol size distribution and chemical composition to the ~~sulfur chemistry module, in each time step. The chemical compounds in SALSA2.0 are~~ Sulfur chemistry module. The aerosol chemical composition in SALSA2.0 is represented by model compound classes ~~: 'sulphate~~'Sulfate' (SU), '~~organic carbon' (OC~~Organic aerosol' (OA), '~~sea~~ Sea salt' (SS), '~~black~~ Black carbon' (BC)~~and 'mineral~~ , and 'Mineral dust' (DU). Of these model compounds, Sulfate, Organic aerosol, and Sea salt constitute the soluble species and are considered as internally mixed in each size bin of the aerosol population. Black carbon and Mineral dust are insoluble species which are externally mixed in each size bin with the soluble species, as described by Kokkola et al. (2018). We consider five different initial conditions with different ~~organic mass fractions , denoted by $\chi_{OA} = \{0.2, 1\}$,~~ OA mass fractions $\chi_{OA} = \{0.2, 0.4, 0.6, 0.8, 1\}$ to represent different environments where OA have been reported in varying concentrations. For example, in boreal forest environments, OA mass fraction is reported around

0.6 0.6 (Äijälä et al., 2019), and in marine environments, around 0.2 (O'Dowd et al., 2004). $\chi_{OA} = 1$ 0.2 (O'Dowd et al., 2004) . $\chi_{OA} = 1$ is a hypothetical extreme where we consider thhe entire aerosol to contain only organic carbonOA to comprise the entire aerosol phase. The initial mass fractions of all aerosol model compounds in these five conditions are shown in Table 2. Here, the sulfur

The Sulfur chemistry module is used to calculate the total sulfate mass aqueous phase secondary Sulfate mass from oxidation of Sulfur dioxide in the aerosol population based on varying hydrogen Hydrogen ion concentration in the aqueous aerosol, considering no organic dissociation, bulk organic dissociation acid dissociation, organic acid dissociation according to well known bulk acidity, and surface modulated organic dissociation. Following this, we use HAMBOX cloud microphysics to calculate CDNC and consequent short-wave radiative effect (RE)for each of these imposed conditions. acid dissociation (Section 2.3 below).

Table 2. Initial aerosol mass fractions of all model compounds in the five different $\chi_{OA} = \{0.2, 1\}$ environmental scenarios considered.

χ_{OA} Organic (χ_{OA})	Sulfate (SU χ_{SU})	Organic (OC) Black carbon (BC χ_{BC})	Sea salt (SS χ_{SS})	Mineral dust (DU χ_{DU})
0.2 0.2	0.4 0.4	0.2 0.05	0.05 0.1	0.1 0.25 0.25
0.4 0.4	0.4 0.4	0.4 0.05	0.05 0.05	0.05 0.1 0.1
0.6 0.6	0.4 0.4	0.6 0	0 0	0 0 0
0.8 0.8	0.2 0.2	0.8 0	0 0	0 0 0
1 1	0 0	1 0	0 0	0 0 0

2.2 Cloud microphysics in HAMBOX

From the total aerosol mass and composition, the resulting cloud droplet number concentrations and consequent short-wave radiative effect are calculated with the HAMBOX cloud microphysics module. The HAMBOX cloud microphysics used in this work includes the calculation of critical supersaturation (S_i) and the activated fraction (n_i) for each aerosol size bin i. A detailed description of the parameterizations and equations used to derive calculate these cloud activation factors are available in from Abdul-Razzak (2002) and Abdul-Razzak et al. (1998) and briefly summarized here.

First, the maximum critical supersaturation (S_{max}) for the air parcel is calculated by as

$$s_max S_{max} = \frac{S_e}{\left[0.5\left(\frac{\varsigma}{\eta}\right)^{3/2} + \left(\frac{S_e^2}{\eta+3\varsigma}\right)^{3/4}\right]^{1/2}}, \quad (1)$$

where η is the surface tension correction factor~~and~~ , ζ is the correction factor for the Kelvin term in the Köhler curve (for details, see ~~Eqs 5 and 6~~ eqs. 5 and 6 in Abdul-Razzak and Ghan (2002)).~~.~~ , and S_e is the effective critical supersaturation for the air parcel,

$$s_e S_e^{2/3} = \frac{\sum_{i=1}^{I} N_i}{\sum_{i=1}^{I} N_i / S_i^{2/3}}. \tag{2}$$

Here~~i is the number of bins~~, ~~S_i is the critical supersaturation for each bin, and~~ $I = 10$ is the total number of aerosol size bins, N_i is the number of particles in each bin ~~, i~~, and S_i is the critical supersaturation for each bin, given by

$$S_i = \exp\left(\frac{A}{D_{\text{wet}}} - \frac{B}{D_{\text{wet}}^3 - d_p^3}\right) - 1, \tag{3}$$

where D_{wet} and d_p are droplet ~~diameter~~ and dry particle ~~diameter~~diameters, respectively. The terms ~~A and B~~ A and B are calculated as

$$kel_A B A = \frac{4 M_w \sigma_w}{R T \rho_w}, \quad B = \frac{6 n_s M_w}{\pi \rho_w}, \tag{4}$$

where ~~M_w~~ $M_w = 0.018$ $\mathrm{kg\,mol^{-1}}$ is the molecular weight of water~~= 0.018 , σ_w~~ , $\sigma_w = 0.073$ $\mathrm{N\,m^{-1}}$ is the surface tension of pure water~~= 0.073 , ρ_w = 1000~~ , $\rho_w = 1000$ $\mathrm{kg\,m^{-3}}$ is the density of water, ~~R = 8.314 , temperature T = 293~~ $R = 8.314$ $\mathrm{J\,K^{-1} mol^{-1}}$ is the ideal gas constant, $T = 293$ K is the temperature, and n_s is the number of moles of solute obtained from the mass fractions of soluble species χ_{OA}, χ_{SU}, and χ_{SS}.

~~Once~~ With the maximum supersaturation of the air parcel~~is determined, the activation of~~ , cloud droplet activation in each bin is determined by comparing $S_{\max}$ with S_{il} and S_{iu} (the lower and upper critical supersaturation bounds of the bin). The number of activated particles ~~(n_i)~~ in each size bin ~~(i)~~ is given by

$$n_i = 0, \quad \text{if} \quad S_{\max} < S_{il}, \tag{5}$$

$$n_i = \frac{\log(S_{\max}/S_{il})}{\log(S_{iu}/S_{il})}, \quad \text{if} \quad S_{il} \le S_{\max} \le S_{iu}, \tag{6}$$

and

$$n_i = 1, \quad \text{if} \quad S_{iu} < S_{\max}. \tag{7}$$

~~S_{il} and S_{iu}~~ S_{il} and S_{iu} are obtained using ~~equation~~ eq. 3 for the diameters of the smallest ~~particle (d_{il}) and biggest particle (d_{iu})~~ (d_{il}) and largest (d_{iu}) particles in each size bin. The average activated fraction for all size bins ~~(n)~~ is then calculated by

$$n = \frac{\sum n_i}{\sum N_i}. \tag{8}$$

The total number of ~~activating~~ activated particles is given by the cloud droplet number concentration~~(CDNC)~~, which is calculated using the number of activating particles within each size bin, as

$$\text{CDNC} = \sum_{i=1}^{I} N_i n_i. \tag{9}$$

The CDNC calculated using ~~equation 9 accounting for organic~~ eq. 9 considering organic bulk acidity and surface modulated organic acid dissociation is denoted by ~~$\mathrm{CDNC_{HA}}$~~ $\mathrm{CDNC_{HA}}$ and the change ~~in CDNC (ΔCDNC)~~ with respect to ~~no organic dissociation ($\mathrm{CDNC_0}$) is~~ the reference condition of no organic acid dissociation ($\mathrm{CDNC_0}$) is

$$\Delta\mathrm{CDNC}\mathrm{CDNC} = \frac{\mathrm{CDNC_{HA}} - \mathrm{CDNC_0}}{\mathrm{CDNC_0}} \frac{\mathrm{CDNC_{HA}} - \mathrm{CDNC_0}}{\mathrm{CDNC_0}}. \tag{10}$$

We estimate the change in short-wave radiative effect (RE) from ~~the change in sulfate mass as a consequence of~~ including organic bulk acidity and surface modulated organic ~~acidity~~acid dissociation, respectively, using the method given by Bzdek et al. (2020) . The change in cloud-top albedo ~~(Δa)~~ at constant cloud liquid water content (~~LWC = 0.03~~ $\mathrm{LWC} = 0.03$ $\mathrm{g\,m^{-3}}$, Thompson (2007)) is calculated from ~~the change in CDNC (ΔCDNC) following Bzdek et al. (2020)~~ ΔCDNC as

$$\Delta a = \mathrm{LWC}\mathrm{LWC}(1 - \mathrm{LWC}\mathrm{LWC})\Delta\mathrm{CDNC}\Delta\mathrm{CDNC}/(3\mathrm{CDNC}\ \mathrm{CDNC}). \tag{11}$$

The short-wave radiative effect ~~(RE)~~ is then calculated as

$$\mathrm{RE}\mathrm{RE} \approx -\mathrm{F_0E_{LWC}}_{\mathrm{LWC}}\mathrm{T_{LWC}}_{\mathrm{LWC}}{}^2\Delta\mathrm{a}, \tag{12}$$

where $F_0 = 340\ \mathrm{W\,m^{-2}}$ is the incoming solar flux at the top of the atmosphere~~. In Equation 12, $E_{\mathrm{LWC}} = 0.3$~~ , $E_{\mathrm{LWC}} = 0.3$ is the fractional coverage of different types of clouds, and ~~$T_{\mathrm{LWC}} = 0.76$~~ $T_{\mathrm{LWC}} = 0.76$ is the transmittance of the atmosphere at visible wavelengths, which is assumed to be constant for all simulations. ~~For the default~~

For all HAMBOX cloud microphysics calculations, ~~cloud temperature is taken as 271 K~~we assume a constant cloud temperature of 271 K, cloud pressure ~~is 101 kPa~~of 101 kPa, cloud fraction ~~is 0.3~~of 0.3, saturation ratio of gas phase water ~~is 0.3~~of 0.3, and updraft velocity ~~is 0.3 . The simulation time for all calculations was taken as 1 hour with 1 second time steps.~~ of 0.3 $\mathrm{m\,s^{-1}}$, consistent with Tegen et al. (2019).

2.3 Sulfur chemistry in HAMBOX

We use the aqueous ~~sulfur~~ Sulfur chemistry module of Feichter et al. (1996b)~~(~~, with modifications described below~~)~~ , to calculate the ~~total sulfate concentration ()~~ aqueous phase secondary Sulfate concentration $[\mathrm{SO_4^{2-}}]''$ in the aerosol population formed from the oxidation of $\mathrm{SO_2}$ by $\mathrm{H_2O_2}$ and $\mathrm{O_3}$ in ~~the~~ aqueous droplets. The reaction rate for the $\mathrm{H_2O_2}$ oxidation pathway can be written as:

$$\frac{\partial}{\partial t}\left[\mathrm{SO_4^{2-}}\mathrm{SO_4^{2-}}\right]'' = \frac{k_4\,[\mathrm{H_2O_2}]\,[\mathrm{SO_2}]}{[\mathrm{H^+}] + 0.1} \frac{k_4\,[\mathrm{H_2O_2}]\,[\mathrm{SO_2}]}{[\mathrm{H^+}] + 0.1} \tag{13}$$

where the rate constant k_4 is calculated by

$$k_4 = 8 \times 10^4 \exp\left(-3650\left(\frac{1}{T} - \frac{1}{298}\right)\right), \tag{14}$$

where T is the cloud temperature = ~~271~~ 271 K. Equation 13 is known to be pH ~~-~~insensitive (Liu et al., 2020) and is used in this work to determine the ~~total sulfate~~ aqueous secondary Sulfate concentration from the $\mathrm{H_2O_2}$ oxidation for simulations where organic acid dissociation is not considered.

To calculate ~~the total sulfate concentration~~ $[SO_4^{2-}]''$ from the H_2O_2 oxidation pathway accounting for pH dependency arising from organic ~~dissociation and further surface modulated organic acidity,~~ bulk acidity, we follow the procedure given by ~~Liu et al. (2020)~~Liu et al. (2020), which is valid for ~~>2. Here~~pH > 2. Here, we use the general acid catalysis reaction mechanism, where SO_2 in an aqueous environment exists as the HSO_3^- anion and reacts with H_2O_2 in the presence of an organic acid (HA) catalyst, which acts as a proton donor (Maaß et al., 1999; McArdle and Hoffmann, 1983). Briefly, the overall reaction mechanism ~~may be~~ is represented as

~~HSO_3^-~~$HSO_3^- + $~~$H_2O_2$~~$ \rightleftharpoons $~~$HOOSO_2^-$~~$H_2O_2 \rightleftharpoons HOOSO_2^- + $~~$H_2O$~~$H_2O$ (R1)

and

~~$HOOSO_2^-$~~$HOOSO_2^- + $~~$HA$~~$HA \rightarrow 2$~~$H^+$~~$H^+ + $~~$SO_4^{2-}$~~$SO_4^{2-} + $~~$X^-$~~$A^-$. (R2)

The rate expression for ~~R1-R2 is~~ R1–R2 is

$$\frac{\partial}{\partial t}\left[\text{~~}SO_4^{2-}\text{~~}SO_4^{2-}\right]'' = \left(k + \frac{k_{HA}[HA]}{[H^+]}\frac{k_{HA}[HA]}{[H^+]}\right) K_{a1}[SO_2][H_2O_2]_{a1}[SO_2][H_2O_2], \quad (15)$$

where K_{a1} is the thermodynamic dissociation constant of H_2SO_3 and k is a constant derived from the reaction rate coefficient and the thermodynamic equilibrium constants. ~~k_{HA}~~ k_{HA} is the overall rate constant for the general acid catalysis mechanism approximated by ~~$\log k_{HA} = -0.57(pK_a) + 6.83$ (Liu et al., 2020; Drexler et al., 1991).~~ $\log k_{HA} = -0.57(pK_a) + 6.83$ (Liu et al., 2020; Drexler et al., 1991). This approximation for k_{HA} in relation to the pK_a of an organic acid was derived by Liu et al. (2020) for an ionic strength of $I = 0.5$ mol kg^{-1}. Therefore, we assume this same ionic strength for aqueous droplets in all our calculations.

The ~~total sulfate~~ secondary Sulfate concentration from O_3 oxidation is given by

$$\frac{\partial}{\partial t}\left[\text{~~}SO_4^{2-}\text{~~}SO_4^{2-}\right]'' = \left(k_{51} + \frac{k_{52}}{[H^+]}\frac{k_{52}}{[H^+]}\right)\left[\text{~~}O_3\text{~~}O_3\right]\left[\text{~~}SO_2\text{~~}SO_2\right], \quad (16)$$

where rate constants k_{51} and k_{52} are calculated ~~by:~~ from

$$k_{51} = 4.39 \times 10^{11} \exp\left(\frac{-4131}{T}\right) \quad (17)$$

and

$$k_{52} = 2.56 \times 10^{3} \exp\left(\frac{-996}{T}\right). \quad (18)$$

Sulfate concentrations thus calculated in the aqueous phase Sulfur chemistry module is distributed to pre-existing aerosol size bins in ~~SALSA2.0~~SALSA2.0.

~~The concentrations in the sulfur chemistry module are obtained from water and aqueous phase sulfate concentrations. Here~~When no organic aerosol acid dissociation (no diss) is considered, the default ~~HAMBOX~~ H^+ concentration in HAMBOX

is denoted by $[H^+]_0$ and ~~gives the concentrations when no organic dissociation (no diss) is considered.~~ obtained from water and aqueous phase Sulfate concentrations as

$$Hconc\left[H^+H^+\right]_{00} = \left[H^+H^+\right]_{initialinitial} + \frac{\left[SO_4^{2-}\right]}{LWC \times MW_{SO_4^{2-}}} \frac{\left[SO_4^{2-}\right]_{sol}}{LWC \times MW_{SO_4^{2-}}}, \quad (19)$$

where ~~LWC is the~~ LWC is the cloud liquid water content in ~~cloud (), is~~ $[g\,m^{-3}]$, $MW_{SO_4^{2-}}$ is the molar weight of the Sulfate anion ($g\,mol^{-1}$), and the soluble Sulfate concentration $[SO_4^{2-}]_{sol}$ is obtained from the summation of soluble ~~sulfate~~ Sulfate (obtained from χ_{SU}, Table 2) in all bins. ~~$MW_{SO_4^{2-}}$ is the molar weight of the sulfate anion (). $[H^+]_{initial}$ is the hydrogen $[H^+]_{initial} = 2.5 \times 10^{-6}$ mol L^{-1}~~ is the Hydrogen ion concentration obtained from the cloud ~~(~~$pH = 5$, which is assumed to be uniform for all ~~bins) set to~~ size bins and consistent with the pH ~~=5, giving initial hydrogen ion concentration () of 2.5×10^{-6}~~ of warm low lying tropospheric clouds (Pye et al., 2020). For all simulations in the ~~sulfur~~ Sulfur chemistry module, we assume $[SO_2]$, $[H_2O_2]$, and $[O_3]$ in cloud are fixed at ~~5 ppb, 1 ppband 50~~ 5 ppb, 1 ppb, and 50 ppb, respectively (Tilgner et al. (2021b)).

We introduce organic ~~dissociation and modify equation (19) to get the total hydrogen~~ acid dissociation to the Sulfur chemistry module by modifying eq. 19 to obtain the total Hydrogen ion concentration in the aerosol population ~~,~~ as

$$\left[H^+H^+\right]_{tot} = \left[H^+H^+\right]_{initialinitial} + \frac{\left[SO_4^{2-}\right]}{LWC \times MW_{SO_4^{2-}}} \frac{\left[SO_4^{2-}\right]_{sol}}{LWC \times MW_{SO_4^{2-}}} + \left[H^+H^+\right]_{HAHA}, \quad (20)$$

where $[H^+]_{HA}$ is the concentration of the ~~hydrogen~~ Hydrogen ions dissociated by the ~~OA.~~

~~The relative change in hydrogen ion concentration (), with respect to 'no diss' is given by~~

~~$deltaHconc\Delta\left[H^+\right] = \frac{[H^+]_{tot} - [H^+]_0}{[H^+]_0} \times 100,$~~

~~and the corresponding relative change in sulfate concentration compared to 'no diss' is~~

~~$\Delta\left[SO_4^{2-}\right] = \frac{\left[SO_4^{2-}\right] - \left[SO_4^{2-}\right]_0}{\left[SO_4^{2-}\right]_0} \times 100,$~~

~~where is the sulfate concentration considering organic dissociation and is the sulfate concentration for 'no diss'.~~

~~The $[H^+]_{tot}$ thus calculated is~~ acidic organic aerosol components. The calculated $[H^+]_{tot}$ is then used to obtain the ~~total sulfate~~ aqueous phase secondary Sulfate concentration in the aerosol population from ~~oxidation using~~ SO_2 oxidation by H_2O_2 (eq. 15~~and from~~) and O_3 ~~oxidation using~~ (eq. 16), for varying conditions of organic ~~dissociation (different $[H^+]_{HA}$ from bulk and surface apparent pK_a). The sulfate~~ acid dissociation. The Sulfate concentrations thus obtained gives a modified ~~sulfate~~ Sulfate mass fraction (~~SU in section 2.1 and table~~ χ_{SU}, Section 2.1 and Table 2) in the entire aerosol population.

2.4 Organic acid dissociation

2.5 ~~Organic Dissociation~~

~~The dissociation behavior of~~ We assume the entire OA fraction is comprised of an organic acid and consider two different acids, Malonic acid (a diprotic acid) and Decanoic acid (a monoprotic acid), as examples of important organic aerosol components in the atmosphere (Yassaa et al., 2001; Narukawa et al., 2002; Mochida et al., 2003; Graham et al., 2003; Cheng et al., 2004; Li and Yu, 2005 with different well known aqueous bulk acidity and prominent examples of moderately and strongly surface active organic species, respectively (Vepsäläinen et al., 2022, 2023). The acid dissociation constants for aqueous bulk solutions are here denoted as pK_a^{bulk} to distinguish the well known bulk dissociation behavior from surface modulated dissociation introduced in Section 2.4.3. The molecular weight (MW), density (ρ), and bulk acid constants for Decanoic and Malonic acids used in our calculations are given in Table 3. For the monoprotic Decanoic acid, pK_a^{bulk} is the reported first pK_a readily available from literature, whereas for the diprotic Malonic acid, pK_a^{bulk} is taken as the sum of the first and second pK_a reported in literature (same as β in eq. 29 below). The dissociation behavior of monoprotic and diprotic acids ~~, under similar dissociation environments , differ greatly from each other and~~ in similar aqueous environments differ greatly and we use different kinetic equations ~~are used to describe them. We consider~~ to describe both treatments of organic ~~dissociation to show two examples of dissociation behavior~~bulk and surface modulated acid dissociation, presented in the following Sections 2.4.1, 2.4.2, and 2.4.3.

2.4.1 ~~Dissociation of monoprotic~~ Monoprotic acids

The dissociation of a monoprotic organic acid (HA) in ~~an aqueous medium may be~~ aqueous solution is represented by the equilibrium

$$\mathrm{HA} + \mathrm{H_2O} \rightleftharpoons \mathrm{A^-} + \mathrm{H_3O^+}, \tag{R3}$$

where $\mathrm{H^+}$ from the dissociation of the organic acid are considered as fully hydrated, such that the concentration of $\mathrm{H_3O^+}$ is equivalent to the concentration of ~~hydrogen~~ Hydrogen ions from dissociation of HA.

The equilibrium acid dissociation constant is

$$K_a = \frac{a_{\mathrm{H_3O^+}} a_{\mathrm{A^-}}}{a_{\mathrm{HA}}} \frac{a_{\mathrm{H_3O^+}} a_{\mathrm{A^-}}}{a_{\mathrm{HA}}}, \tag{21}$$

where ~~$a_{\mathrm{H_3O^+}}$, $a_{\mathrm{A^-}}$ and a_{HA}~~ $a_{\mathrm{H_3O^+}}$, $a_{\mathrm{A^-}}$ and a_{HA} are the activities of ~~$\mathrm{H_3O^+}$cations, $\mathrm{A^-}$anions and HA~~ $\mathrm{H_3O^+}$cations, $\mathrm{A^-}$anions and HA molecules, respectively. ~~Eq.~~ Equation 21, can be approximated in terms of the molar concentrations and ideal-dilute molar concentration based activity coefficients (γ_i) of each species i as ~~:~~

$$K_a = \frac{[\mathrm{H_3O^+}][\mathrm{A^-}]}{[\mathrm{HA}]} \frac{\gamma_{\mathrm{H_3O^+}}\gamma_{\mathrm{A^-}}}{\gamma_{\mathrm{HA}}} \frac{[\mathrm{H_3O^+}][\mathrm{A^-}]}{[\mathrm{HA}]} \frac{\gamma_{\mathrm{H_3O^+}}\gamma_{\mathrm{A^-}}}{\gamma_{\mathrm{HA}}}. \tag{22}$$

Since ~~HA is~~ a monoprotic acid ~~with only one ionsizable hydrogen,~~ HA has only one ionizable Hydrogen, in eq. 22

$$[\mathrm{A^-}] = [\mathrm{H_3O^+}], \text{ and } [\mathrm{HA}] = [\mathrm{HA}]_{\mathrm{tot}} - [\mathrm{H_3O^+}], \tag{23}$$

where ~~$[\mathrm{HA}]_{\mathrm{tot}}$~~ $[\mathrm{HA}]_{\mathrm{tot}}$ is the total concentration of the organic acid. The acid dissociation degree α is defined as

$$\alpha = \frac{[\mathrm{A^-}]}{[\mathrm{HA}]_{\mathrm{tot}}} \frac{[\mathrm{A^-}]}{[\mathrm{HA}]_{\mathrm{tot}}} = \frac{[\mathrm{H_3O^+}]}{[\mathrm{HA}]_{\mathrm{tot}}} \frac{[\mathrm{H_3O^+}]}{[\mathrm{HA}]_{\mathrm{tot}}}. \tag{24}$$

~~Combining equations (22) and (24) and approximating~~ $\frac{\gamma_{H_3O^+}\gamma_{F^-}}{\gamma_{HF}}$ Combining eq. 22 and 24 and approximating $\frac{\gamma_{H_3O^+}\gamma_{A^-}}{\gamma_{HA}}$ with the mean activity coefficient $\gamma_{\pm}$,

$$K_{aa} = [HA]_{tot}[HA]_{tot}\left(\frac{\alpha^2}{1-\alpha}\right)\gamma_{\pm}^2. \quad (25)$$

For a highly ~~diluted~~ dilute solution (e.g., ~~$[HA]_{tot}$ <0.001), $\gamma_{\pm}^2$ can be assumed as 1. Under these conditions, equation (25)~~ $[HA]_{tot} < 0.001$ mol L^{-1}), $\gamma_{\pm}^2 \approx 1$ and eq. 25 can be written as

$$\alpha = \frac{-K_a + \sqrt{K_a^2 + 4K_a \times [HA]_{tot}}}{2[HA]_{tot}} \frac{-K_a + \sqrt{K_a^2 + 4K_a \times [HA]_{tot}}}{2[HA]_{tot}}. \quad (26)$$

2.4.2 ~~Dissociation of diprotic acids~~

With $[HA]_{tot}$ known from χ_{OA} and other properties of the aerosol population, the Hydrogen ion concentration from organic acid dissociation $[H^+]_{HA}$ is obtained as $[H_3O^+]$ in eq. 24 by

$$[H^+]_{HA} = [H_3O^+] = \alpha[HA]_{tot}, \quad (27)$$

where the acid dissociation degree α is given by eq. 26.

2.4.2 Diprotic acids

For a diprotic organic acid (H_2A), the dissociation of H^+ ions in an aqueous ~~medium occurs~~ solution can be considered to occur in two stages~~:~~,

$$H_2A H_2A + H_2O \rightleftharpoons HA^- H_2O \rightleftharpoons HA^- + H_3O^+ H_3O^+ \quad (R4)$$

and

$$HA^- HA^- + H_2O \rightleftharpoons A^{2-} H_2O \rightleftharpoons A^{2-} + H_3O^+ H_3O^+. \quad (R5)$$

The dissociation constant for R4 is the first dissociation constant of the diprotic acid, denoted as K_{a1}, and the dissociation constant for R5 is the second dissociation constant of the diprotic acid, denoted as K_{a2}. The overall dissociation constant of ~~the diprotic acid~~ H_2A is

$$\beta = K_{a1}K_{a2}, \quad (28)$$

and therefore,

$$p\beta = pK_{a1} + pK_{a2}. \quad (29)$$

Using similar assumptions as for the monoprotic acid, for a highly dilute solution, the acid dissociation degree α for a diprotic acid can be derived as ~~:~~

$$\alpha = \frac{1}{4\beta[H_2A]_{tot} + 2} \frac{1}{4\beta[H_2A]_{tot} + 2}, \quad (30)$$

where ~~,~~ $[H_2A]_{tot}$ is the total concentration of the diprotic acid. ~~Thus, based on the known pK_a and organic concentrations $[HA]_{tot}$ and $[H_2A]_{tot}$ derived from the OA mass fraction, we calculate the dissociation degree (α) of the organic acids, following which the amount of H^+ ions dissociated by~~ Analogously to the case of a monoprotic acid, the ~~organic acid is calculated for the bulk solution.~~ Hydrogen ion concentration from dissociation of a diprotic organic acid $[H^+]_{HA}$ is given by

$$[H^+]_{HA} = [H_3O^+] = \alpha[H_2A]_{tot}, \tag{31}$$

where the acid dissociation degree α is now given by eq. 30.

2.4.3 ~~van't Hoff factor for~~ Surface modulated organic acid dissociation

~~The dissociation of the solutes influences the available moles of solute in aerosol particles, affecting the water activity and critical supersaturation calculations in the model. The van't Hoff factor for organic dissociation (i_{OA}) is related to the dissociation degree, α (shown in eq. 26 and 30) as~~

~~$vhfactor$~~$i_{OA} = 1 + \alpha(n_{ions} - 1)$,

~~where n_{ions} is the number of ions formed from one formula unit of the organic acid .~~

~~The available moles of the solute n_s in SALSA2.0 is calculated as~~

~~ns~~$n_s = i_{SU}n_{SU} + i_{OA}n_{OA} + i_{SS}n_{SS}$,

We now introduce a simple empirical representation of the shift in organic acid dissociation previously observed in surface-sensitive XPS experiments. Werner et al. (2018) found that the surface specific dissociation state of surface active mono-carboxylic acids was significantly suppressed in dilute aqueous solutions across a very wide range of solution $pH = 2 - 12$. Similar suppressed dissociation states were also found for other mono- and dicarboxylic acids of both stronger and weaker surface activity, in aqueous solutions closer to neutral pH (Prisle et al., 2012b; Werner et al., 2014b; Öhrwall et al., 2015a). The shifted dissociation states are attributed to both increased concentrations of the surface active organic acids in the surface and increased non-ideality (higher activity coefficients) of the charged deprotonated conjugate species A^- and hydronium ions, compared to the neutral molecular acid HA, in the organic-rich air–solution interfacial region (Werner et al., 2018; Prisle, 2023). From eq. 22, this corresponds to an apparent shift of the acid pK_a at the surface,

$$pK_a = pK_a^{bulk} + \log\left(\frac{\gamma_{H_3O^+}\gamma_{A^-}}{\gamma_{HA}}\right), \tag{32}$$

~~where the n_{SU}, n_{OA} and n_{SS} are the initial number of moles of sulfate, organic aerosol and sea salt, respectively, while i_{SU}, i_{OA} and i_{SS} are the corresponding van't Hoff factors. The available molar amount of the solute n_s influences the critical supersaturation of the bins (the Raoult term B in eq. 3) and maximum critical supersaturation S_{max}, thereby affecting the critical supersaturation for each bin (S_i) and consequently the activation processes. In SALSA2.0, the sulfate and sea salt are considered as fully dissociated and i_{SU} and i_{SS} are set to 3 and~~ compared to the well known bulk acidity pK_a^{bulk} obtained for dilute aqueous solutions, where all activity coefficients are assumed to be ideal, $\gamma_i = 1$ (Prisle, 2023).

The dissociation states observed with XPS are broadly consistent with a magnitude of the apparent shift in pK_a of $\log\left(\frac{\gamma_{H_3O^+}\gamma_{A^-}}{\gamma_{HA}}\right) = 1 -$ pH units across the surface titration curve (Prisle, 2023). We here introduce the effect of surface modulated acid dissociation by shifting the well known bulk pK_a of each organic acid according to these shifts of the surface titration curves. We consider two magnitudes of this apparent shift, covering the range of experimental observations from XPS. For a monoprotic acid, we consider $pK_a = pK_a^{\mathrm{bulk}} + 1$ and $pK_a = pK_a^{\mathrm{bulk}} + 2$, where pK_a^{bulk} is the well known pK_a of the organic acid in aqueous bulk solution. To represent the surface shifted dissociation of both carboxylic groups in a diprotic acid, we increase both the first and second acid constant, by 1 or 2 , respectively. By default, organic aerosol is not considered as dissociated and i_{OA} is set equal to 1. Here, we assume that the entire organic aerosol is an organic acid and the i_{OA} is calculated using eq. 34, for the surface and bulk representation of organic dissociation . The total available moles of solute (n_s, eq. 33) is thus modified for organic dissociation and is then reflected in the Raoult term, B (eq. 4) which changes the critical supersaturation S_i for each bin. The change in Raoult term and S_i from inclusion of organic dissociation in van't Hoff factor, i_{OA}, pH units, to similarly obtain $pK_a^{\mathrm{bulk}} + 1$ and $pK_a^{\mathrm{bulk}} + 2$. We here refer to the shifted pK_a values as the surface modulated *apparent* pK_a. However, we strongly emphasize that the pK_a, which is an intrinsic property of each organic acid in bulk aqueous solution, is independent of the kinetic driven sulfate concentrations in the aqueous aerosol, and is instead a measure of the change in water activity due to the dissociation not itself changed. Only the dissociation responses of the organic acid and the consequent increase in the number of available moles of solute, $n_s$acids to a given pH of the solution (here, the cloud pH) are changed in the surface (Prisle, 2023).

2.4.4 Representation of bulk and surface modulated organic dissociation

We assume the entire OA to be an organic acid and consider it to be dissociated according to α calculated using reported pK_a values from literature, using eqs. 26 and 30 for monoprotic and For both mono- and diprotic acids, respectively. This representation of organic dissociation does not account for any surface specific effects and represents organic dissociation in the aqueous aerosol bulk, and is denoted as pK_a^{bulk}. For the monoprotic acid pK_a^{bulk} is the reported first the values used for surface modulated apparent pK_a readily available from literature, whereas are given in Table 3. For each pK_a, the corresponding acid dissociation degree α is calculated for the monoprotic acid using eq. 26 and for the diprotic acid , the sum of the reported first and second using eq. 30. The value for α decreases with increasing pK_a, such that the increased apparent pK_a , available in literature, is taken as pK_a^{bulk} (same as $p\beta$, eq. 29).

Previous work has shown that for aerosol particles comprising surface active organic acids and their salts, such as sodium octanoate, sodium decanoate, sodium dodecanoate, and sodium dodecyl sulfate, during major part of hygroscopic growth and cloud droplet activation, almost all surface active OA is partitioned to the surface (Prisle et al., 2010b, 2011; Lin et al., 2018, 2020; Prisle, 2 . For spherical droplets of diameter D_{wet}=0.1, 1, and 10 , the surface area to bulk volume ratio ($A/V = 6/d$) is 60, 6, and 0.6 , respectively (Prisle et al., 2010b). Given the high A/V of small droplets, such as submicron activating aqueous aerosols, and the surface propensity of atmospherically relevant organic acids , surface specific properties may significantly contribute to, or entirely dominate, the overall aerosol properties (Prisle et al., 2012b; Prisle, 2021)represent suppressed dissociation of the organic acid in the surface.

~~Werner et al. (2018) investigated the~~ The surface modulation of organic dissociation is most pronounced in a range of several pH units around the bulk pK_a. At very low and very high pH, the surface ~~characteristics of butyric and pentanoic acidin dilute aqueous solution (50 carboxylic acid) using surface-sensitive X-ray Photoelectron Spectroscopy, and found that the acid-base equilibrium was systematically shifted in~~ dissociation states collapse onto the well known bulk solution dissociation behavior (Werner et al., 2018; Prisle, 2023). For both the organic acids used here, the ~~surface, corresponding to an apparent shift in pK_a of the order of 1 to 2~~ pK_a^{bulk} is within a few pH ~~units, compared to the bulk solution. Similar magnitudes of apparent pK_a shift were also previously observed by Prisle et al. (2012b) for dilute aqueous mixtures of decanoate/decanoic acid and by Öhrwall et al. (2015b) for propanoic and octanoic acid solutions. Each of these organic acids showed significant surface propensity in the aqueous solutions. Here, we introduce a simple implementation of the surface specific shift in acid/base equilibrium reported in these studies. We introduce acidity in the whole aerosol using α, and modulate its value to represent observations made in the surface~~ units of the cloud pH.

~~The pK_a are derived by taking the negative logarithm of the acid dissociation constant from eq. 22, and the pK_a^{bulk} and apparent pK_a at the surface~~

Although we implement the effect of surface modulated acid dissociation as a consequence of simultaneous surface activity of the organic acid, ~~pK_a^{surf}, are related as~~

$$pK_a^{\mathrm{surf}} = pK_a^{\mathrm{bulk}} + \log\left(\frac{\gamma_{\mathrm{H_3O^+}}\gamma_{\mathrm{A^-}}}{\gamma_{\mathrm{HA}}}\right),$$

~~where γ_i denotes the activity coefficient of an ideal dilute 1 molar solution of component i. The observed shift in~~ we do not explicitly consider the bulk–surface partitioning of organic acids in our calculations. Our simple empirical representation by shifting the apparent pK_a ~~in the surface can be rationalized in terms of~~ for the organic acid corresponds to assuming that the overall dissociation state in aqueous aerosols and droplets is described by the surface modulated properties. This is closely representative of aerosols and droplets where the majority of organic aerosol components are partitioned to the aqueous surface, as a consequence of strong organic surface activity or high A/V in the ~~factor $\log\left(\frac{\gamma_{\mathrm{H_3O^+}}\gamma_{\mathrm{A^-}}}{\gamma_{\mathrm{HA}}}\right)$, reflecting the increased non-ideality of the charged deprotonated species () and hydronium ions, compared to the neutral molecular acid (), in the surface. The magnitude of~~ microscopic and submicron size ranges (Prisle, 2021, 2023). In real atmospheric aerosol and droplet mixtures of both surface active and more water soluble OA, organic species will be partially partitioned to the ~~1 – 2 units shift in $\log\left(\frac{\gamma_{\mathrm{H_3O^+}}\gamma_{\mathrm{A^-}}}{\gamma_{\mathrm{HA}}}\right)$ further depends on the increased concentrations of the organic acid conjugate pair in the surface driven by bulk-surface partitioning (Prisle et al., 2012b; Öhrwall et al., 2015b; Werner et al., 2018).~~ surface and the overall dissociation state should be described as a combination of both well known bulk acidity and surface modulated states. The present simple empirical representation therefore gives an upper bound of the potential effects of surface modulated acid dissociation according to the previous observations from XPS experiments.

~~We here consider two values of~~ When surface modulated organic acid dissociation is considered, these properties are assumed to remain consistent throughout the 1-hour simulations. Prisle et al. (2008) and Prisle (2021) estimated that surface adsorption of typical atmospheric surfactants equilibrate within a timescale of a second in micron-sized droplets. Lin et al. (2020) investigated the impact of surface adsorption dynamics on surfactant effects in cloud droplet activation and found that different

dynamic effects nearly cancel out at every time step. Noziere et al. (2014) assumed that both the bulk and surface reach a state of reasonable equilibrium with respect to organic adsorption at the aqueous surface within approximately 495 seconds. Therefore, we consider this assumption to be a reasonable first approximation.

Table 3. Properties of the organic acids used in calculations of acid dissociation, including molecular properties (MW and ρ), well known bulk solution acidity (pK_{a1}, pK_{a2}, and pK_a^{bulk}), and surface modulated dissociation properties (implemented as $pK_a^{\mathrm{bulk}}+1$ and $pK_a^{\mathrm{bulk}}+2$).

	Malonic acid	Decanoic acid
Molecular weight, MW	104 $\mathrm{g\,mol^{-1}}$	172.26 $\mathrm{g\,mol^{-1}}$
Density, ρ	1.62 $\mathrm{g\,cm^{-3}}$	0.893 $\mathrm{g\,cm^{-3}}$
pK_{a1}	2.8[a]	4.9[b]
pK_{a2}	5.7[a]	-
pK_a^{bulk}	8.5	4.9
$pK_a^{\mathrm{bulk}}+1$	10.5	5.9
$pK_a^{\mathrm{bulk}}+2$	12.5	6.9

[a] Stahl and Wermuth (2002). [b] Martell and Smith (1974).

2.4.4 The van't Hoff factor for organic dissociation

Aqueous phase dissociation also influences the available amount of solute species in aerosol particles and droplets, affecting the calculations of water activity and critical supersaturation (Section 2.2). The molar amount of available solute n_s is calculated in SALSA2.0 from the the ~~apparent shift, covering the range of observations,~~ molar amounts of all the internally mixed soluble species as

$$n_s = i_{\mathrm{SU}} n_{\mathrm{SU}} + i_{\mathrm{OA}} n_{\mathrm{OA}} + i_{\mathrm{SS}} n_{\mathrm{SS}}, \tag{33}$$

where the n_{SU}, n_{OA} and n_{SS} are the molar amounts of Sulfate, Organic aerosol, and Sea salt, respectively, derived from the initial aerosol mass fractions given in Table 2 and i_{SU}, i_{OA} and ~~representing stronger or less strong influence of surface properties on the whole droplet. For the monoprotic acid, pK_a^{bulk}+1 and pK_a^{bulk}+2 were extrapolated from the reported pK_a. To represent the surface shifted dissociation of both carboxylic groups in~~ i_{SS} are the corresponding van't Hoff factors for each soluble species. In SALSA2.0, the ~~diprotic acid, we increase both the first and second pK_a by one unit for pK_a^{bulk}+1, and~~

~~by two units for pK_a^{bulk}+2. For each of the apparent pK_a, the corresponding dissociation degree (~~Sulfate and Sea salt are considered as fully dissociated, such that $i_{\mathrm{SU}} = 3$ and $i_{\mathrm{SS}} = 2$. By default, Organic aerosol is not considered as dissociated and $i_{\mathrm{OA}} = 1$.

To include effects of organic acid dissociation, i_{OA} is calculated with consideration of the acid dissociation degree α ~~) is calculated~~ (from eq. 26 and 30) as

$$i_{\mathrm{OA}} = 1 + \alpha(n_{\mathrm{ions}} - 1), \tag{34}$$

where $n_{\mathrm{ions}} = 2$ for the monoprotic acid ~~using eq. 26 and~~ and $n_{\mathrm{ions}} = 3$ for the diprotic acid~~using eq. 30. α is smaller with increasing pK_a, and therefore the shifted acidity in the surface represents suppressed organic dissociation.~~ , is the number of ions formed from one formula unit of the organic acid. The total available molar amount of solute (n_s, eq. 33) is thus modified by organic acid dissociation according to i_{OA} from eq. 34 and reflected in the Raoult term B (eq. 4) which changes the critical supersaturation S_i for each aerosol size bin.

The van't Hoff factor is calculated for each ~~apparent~~ pK_a using eq. 34. The dissociation degrees and van't Hoff factors for the no organic dissociation (no diss), ~~bulk organic dissociation~~ organic acid dissociation according to bulk acidity (pK_a^{bulk}) and surface modulated suppressed organic ~~dissociation (pK_a^{bulk}+1 and pK_a^{bulk}+2~~acid dissociation ($pK_a^{\mathrm{bulk}} + 1$ and $pK_a^{\mathrm{bulk}} + 2$), for all the OA mass fractions considered here are given in the ~~appendix (Table ??~~Supplement (Table S1).

~~We use two different organic acids as examples, malonic acid (a diprotic acid) and decanoic acid (a monoprotic acid), as they are important aerosol components in the atmosphere (Narukawa et al., 2002; Tedetti et al., 2006; Prisle et al., 2012b) and prominent examples of moderately and strongly surface active species, respectively (Vepsäläinen et al., 2022). The molecular weight, density and pK_a^{bulk} values available from literature, as well as the surface modulated pK_a^{bulk}+1 and pK_a^{bulk}+2, for decanoic acid and malonic acid , are given in Table 3.~~

~~Properties of the organic acids used in all model simulations of the organic acids. Malonic acid Decanoic acid Molecular weight 104 172.26 Density, ρ 1.62 0.893 pK_{a1} 2.8[a] 4.9[b] pK_{a2} 5.7[a] - pK_a^{bulk} 8.5 4.9 pK_a^{bulk}+1 10.5 5.9 pK_a^{bulk}+2 12.5 6.9~~

3 ~~Results and discussions~~

~~We present the results of the HAMBOX-sulfur chemistry calculations~~

3 Results and discussions

We present the results of HAMBOX simulations for Sulfur chemistry, cloud microphysics, and aerosol-cloud-climate effects, considering organic acid bulk acidity (pK_a^{bulk}), surface modulated suppressed organic acid dissociation ($pK_a^{\mathrm{bulk}} + 1$ and 2), and no organic acid dissociation (no diss). Simulations were carried out with the entire OA fraction (Table 2) as either Malonic (OA = Malonic acid) or Decanoic (OA = Decanoic acid) acid. Results of Sulfur chemistry calculations are presented in terms of total ~~hydrogen ion concentration ,~~ Hydrogen ion concentration $[\mathrm{H}^+]_{\mathrm{tot}}$ ~~, and total sulfate concentration , ,~~ and secondary Sulfate concentration $[\mathrm{SO}_4^{2-}]''$ in the aerosol population~~, accounting for bulk organic dissociation, surface modulated suppressed~~

~~organic dissociation and no organic dissociation~~. The consecutive effect on cloud activating properties ~~,~~ is then presented in terms of change in ~~CDNC (~~cloud droplet number concentration ΔCDNC ~~) and RE, compared to no organic dissociation is then presented for bulk dissociation~~ and cloud radiative effect RE predicted for bulk and surface modulated suppressed dissociation of the ~~organics. Aqueous aerosol hydrogen ion concentration, , calculated with the sulfur chemistry module of HAMBOX for the whole aerosol population with droplet radius 0.317 to 40 , after 1 hour of simulation time, assuming five different initial organic mass fractions ($\chi_{OA} = \{0.2, 1\}$), denoted by different colors (see also Table 2), from equation 20 with varying apparent pK_a = pK_a^{bulk}+X, corresponding to representations of bulk (X=0) and surface modulated (X=1 and X=2) organic dissociation. (a, b) All OA is assumed as Malonic acid. (c, d) All OA is assumed as Decanoic acid. The 'no diss' represents simulation without accounting for organic dissociation, and sub-figures b and d show the relative change in with respect to the 'no diss', Δ [H$^+$], calculated using eq. 35.~~ organic acids, compared to no organic dissociation.

3.1 Aqueous aerosol Hydrogen ion concentration

Figure 1 shows the ~~aqueous aerosol hydrogen ion concentration (~~total Hydrogen ion concentration $[H^+]_{tot}$ ~~)~~ calculated with HAMBOX ~~using (~~eq. 20) in the aqueous aerosol population with sizes between $D_{wet} = 0.317 - 40$ µm after 1 hour of simulation time, as a function of varying ~~apparent~~ pK_a~~= pK_a^{bulk}+X~~, corresponding to representations of bulk (~~X=0~~pK_a^{bulk}) and surface modulated (~~X=1 and 2) organic~~ $pK_a^{bulk} + 1$ and 2) organic acid dissociation, considering ~~(~~OA = Malonic acid (panels a, b), and OA = ~~malonic acid , and (~~Decanoic acid (panels c, d)~~OA = decanoic acid~~, for varying initial mass fraction of organic aerosol (~~$\chi_{OA} = \{0.2, 1\}$ in different colours~~$\chi_{OA} = \{0.2, 0.4, 0.6, 0.8, 1\}$ in blue, purple, pink, orange, and yellow, respectively). The ~~hydrogen~~ Hydrogen ion concentration with no organic dissociation (~~obtained using~~ no diss, eq. 19) is also shown as a black line. As expected, ~~the hydrogen ion concentration in the aerosol~~ $[H^+]_{tot}$ does not change with ~~apparent~~ pK_a when organic acid dissociation is not accounted for, whereas a significant increase ~~in hydrogen ion concentration is observed when organic~~ is observed for both Malonic and Decanoic acids when organic acid dissociation is considered~~for both organic acids. The hydrogen~~ . The total Hydrogen ion concentration is highest when ~~bulk organic~~ organic acid dissociation is considered ~~(~~according to pK_a^{bulk} ~~) for all initial OA mass fractions, and decreases as OA~~ and decreases for all χ_{OA} as acid dissociation is increasingly suppressed according to the surface modulated ~~acidity in the form of increasing apparent pK_a.~~ apparent $pK_a^{bulk} + 1$ and $pK_a^{bulk} + 2$.

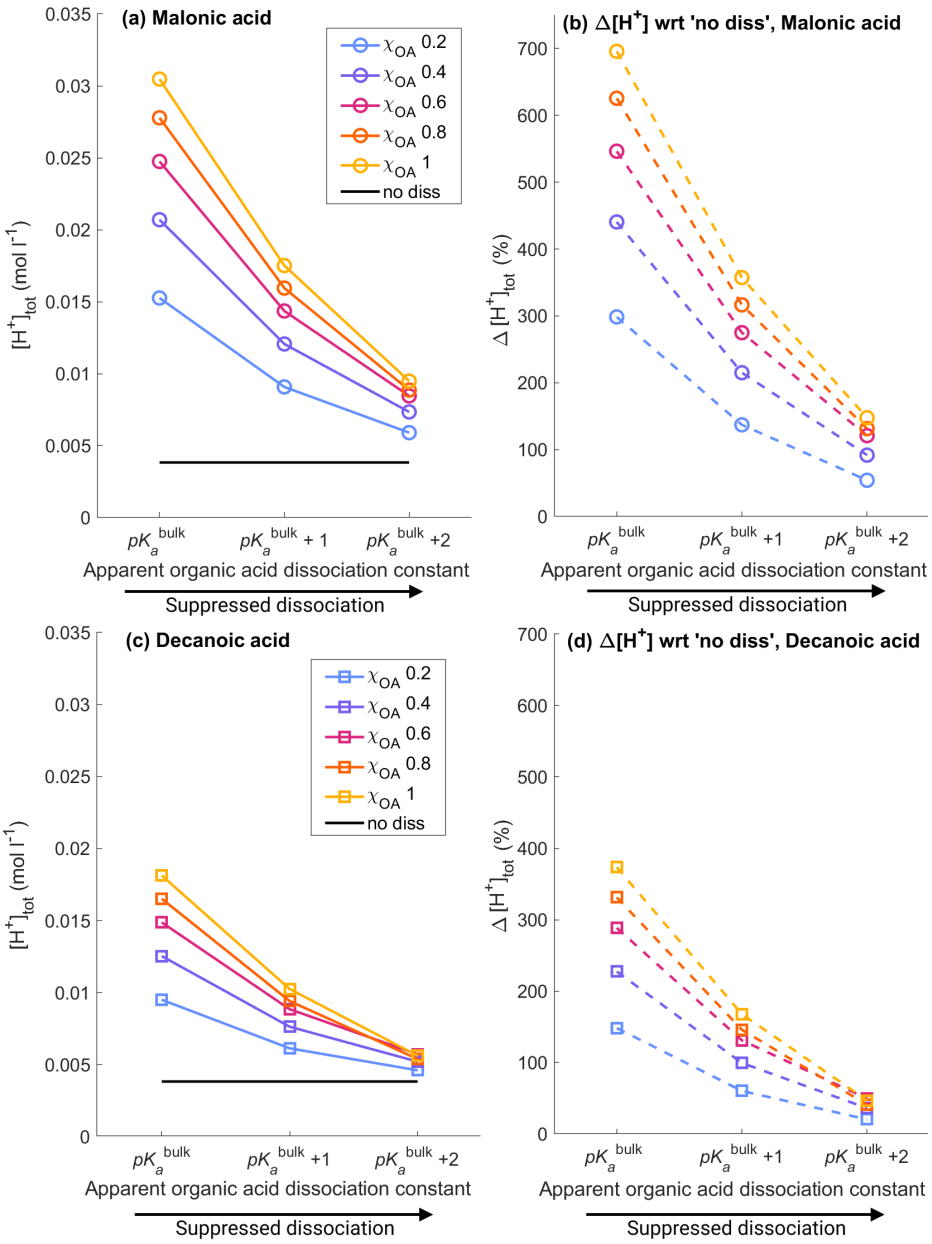

Figure 1. Aqueous aerosol total Hydrogen ion concentration, $[\mathrm{H}^+]_{\mathrm{tot}}$, calculated from eq. 20 with the Sulfur chemistry module of HAMBOX in the aqueous aerosol population with sizes between $D_{\mathrm{wet}} = 0.317 - 40$ µm, after 1 hour of simulation time, assuming five different initial organic mass fractions $\chi_{\mathrm{OA}} = \{0.2, 0.4, 0.6, 0.8, 1\}$, denoted by blue, purple, pink, orange, and yellow, respectively (see also Table 2), with varying pK_a corresponding to representations of bulk (pK_a^{bulk}) and surface modulated ($pK_a^{\mathrm{bulk}} + 1$ and 2) organic acid dissociation. (a, b) All OA is assumed to be Malonic acid, and (c, d) all OA is assumed to be Decanoic acid. Simulations without accounting for organic acid dissociation are represented by 'no diss' and panels b and d show the relative change in total Hydrogen ion concentration $\Delta[\mathrm{H}^+]_{\mathrm{tot}}$ calculated from eq. 35 for each of the acid dissociation conditions with respect to 'no diss'.

The relative change in ~~hydrogen ion concentration compared to~~ total Hydrogen ion concentration with respect to the 'no diss' ~~($\Delta[H^+]$) for malonic acid is 298.5%~~ condition

$$\Delta\left[H^+\right]_{tot} = \frac{[H^+]_{tot} - [H^+]_0}{[H^+]_0} \times 100, \quad (35)$$

is shown for Malonic and Decanoic acids in panels (b) and (d), respectively, of fig. 1. For Malonic acid with pK_a^{bulk} ~~for~~ , $\Delta[H^+]_{tot} = 298.5\%$ at the lowest OA mass fraction ~~(χ_{OA} 0.2) and 696~~ $\chi_{OA} = 0.2$ and 696% for the highest OA mass fraction ~~(χ_{OA} 1). Under~~ $\chi_{OA} = 1$. Under the surface modulated suppressed organic ~~dissociation of pK_a^{bulk}+1, the $\Delta[H^+]$ decreases to 137% and 357% , respectively, for χ_{OA} 0.2 and χ_{OA} 1.~~ acid dissociation condition $pK_a^{bulk} + 1$, $\Delta[H^+]_{tot}$ decreases to 137% and 357% for $\chi_{OA} = 0.2$ and $\chi_{OA} = 1$, respectively. On further suppression of organic ~~dissociation with pK_a^{bulk}+2, these values~~ acid dissociation according to $pK_a^{bulk} + 2$, $\Delta[H^+]_{tot}$ further decrease to ~~54% and 148~~54% and 148%, respectively~~. The hydrogen ion concentration for decanoic acid~~ , at these OA mass fractions. For Decanoic acid organic aerosol, the total Hydrogen ion concentration at pK_a^{bulk} ~~, increases by 148~~increases by 148% with respect to 'no diss' for ~~χ_{OA} 0.2 and by 374% for χ_{OA} 1. At pK_a^{bulk}+1, these values decrease to 61% and 168~~ $\chi_{OA} = 0.2$ and by 374% for $\chi_{OA} = 1$. At $pK_a^{bulk} + 1$, $\Delta[H^+]_{tot}$ decreases to 61% and 168%, respectively, and at ~~pK_a^{bulk}+2, they further decrease to 20% and 47% for χ_{OA} 0.2 and 1~~ $pK_a^{bulk} + 2$ further to 20% and 47% for $\chi_{OA} = 0.2$ and 1, respectively. Therefore, ~~on considering~~ even considering the stronger surface modulated suppression of organic ~~dissociation with pK_a^{bulk}+2~~acid dissociation with $pK_a^{bulk} + 2$, the total ~~hydrogen~~ Hydrogen ion concentration in the aqueous aerosol is still ~~20 to 47~~20 – 47% higher than 'no diss' for ~~decanoic~~ Decanoic acid, and ~~54 to 148% for malonic~~ 54 – 148% higher for Malonic acid, depending on the initial organic aerosol mass fraction. ~~Aqueous aerosol sulfate concentrations () for malonic acid (sub-figures a, c) and decanoic acid (sub-figures b, d), obtained from oxidation of sulfur dioxide by (using eq. 15 and 13) and (using eq. 16), as a function of varying apparent pK_a^{bulk}+X, corresponding to representations of bulk (X=0) and surface modulated (X=1 and 2) organic dissociation, calculated in the sulfur chemistry module of HAMBOX for the whole aerosol population with droplet radius 0.317 to 40 , after 1 hour of simulation time, assuming five different initial organic mass fractions (χ_{OA}), denoted by different colors (see also Table 2). The 'no diss' represents simulation without accounting for organic dissociation.~~

~~Figure ?? shows the sulfate concentrations () produced through~~

The results shown in fig. 1 and in the following are obtained for a constant ionic strength of $I = 0.5$ mol kg^{-1}. Ionic strength is a bulk solution phenomenon and not expected to affect surface adsorbed organic acids, which can be considered as a (partially) liquid-liquid separated phase (Prisle et al., 2010a), to the same degree as in the bulk solution. Therefore, the amount of Hydrogen ions dissociated by the organic acid ($[H^+]_{HA}$, eq. 20) is expected to depend on I mainly for the bulk solution condition and potentially to some extent for the surface modulated conditions. The total Hydrogen ion concentration ($[H^+]_{tot}$, eq. 20) in the aerosol population is shown in fig. S1 of the Supplement for OA = Malonic acid, considering $\chi_{OA} = 0.4$ and 0.6, and for varying ionic strengths $I = \{0.5, 1, 3, 5\}$ mol kg^{-1}.

The total Hydrogen ion concentration decreases with increasing ionic strength, as expected. For $\chi_{OA} = 0.4$, $[H^+]_{tot}$ is approximately 270% greater for pK_a^{bulk} than without consideration of dissociation (no diss) at $I = 5$ mol kg^{-1}. For the surface modulated dissociation condition at the same ionic strength and organic aerosol mass fraction, $[H^+]_{tot}$ is approximately 120%

greater for $pK_a^{\text{bulk}} + 1$ compared to 'no diss'. Even for the more strongly suppressed dissociation corresponding to $pK_a^{\text{bulk}} + 2$, $[H^+]_{\text{tot}}$ is approximately 45% higher than without dissociation. Therefore, for $I = \{0.5, 1, 3, 5\}$ mol kg^{-1}, the total Hydrogen ion concentration in the aqueous aerosol has significant contribution from organic acid dissociation. Similar analysis for varying ionic strength considering OA = Decanoic acid was not immediately possible, due to lack of data on the variation of pK_a with I for aqueous Decanoic acid solutions. However, measurements of pK_a for Acetic acid in aqueous solutions with varying ionic strength were reported by Cohn et al. (1928). The total Hydrogen ion concentration for varying ionic strengths in the aqueous aerosol is shown for OA = Acetic acid in fig. S2 of the Supplement. For OA = Acetic acid, organic acid dissociation considering $I = \{0.02, 0.2, 1, 4\}$ mol kg^{-1} results in approximately $270 - 380\%$ higher $[H^+]_{\text{tot}}$ than without acid dissociation. Both Acetic acid ($pK_a = 4.76$, Goldberg et al. (2002)) and Decanoic acid ($pK_a = 4.9$, Martell and Smith (1974)) are straight chain monocarboxylic acids with comparable bulk acidity and their aqueous dissociation properties are expected to be similar. Therefore, variation in I is expected to result in similar $[H^+]_{\text{tot}}$ in the aqueous aerosol for OA = Decanoic acid as for OA = Acetic acid.

3.2 Aqueous aerosol Sulfate concentration

Figure 2 shows the aqueous phase secondary Sulfate concentrations $[SO_4^{2-}]''$ from oxidation of SO_2 by H_2O_2 and O_3 (Section 2.3) ~~for the whole~~ in the aqueous aerosol population with ~~droplet radius 0.317~~ sizes between $D_{\text{wet}} = 0.317 - 40$ µm~~to 40 , after 1~~, after 1 hour of simulation time, for varying ~~bulk~~ acid pK_a corresponding to representations of bulk (pK_a^{bulk}) and surface modulated ~~pK_a of OA dissociation,~~ ($pK_a^{\text{bulk}} + 1$ and $pK_a^{\text{bulk}} + 2$) organic dissociation, assuming five different initial organic mass fractions $\chi_{\text{OA}} = \{0.2, 0.4, 0.6, 0.8, 1\}$, denoted by blue, purple, pink, orange, and yellow, respectively, and where OA = ~~malonic acid (sub-figures~~ Malonic acid (panels a, c) and ~~decanoic acid (sub-figures~~ Decanoic acid (panels b, d)~~, assuming five different initial organic mass fractions ($\chi_{\text{OA}} = \{0.2, 1\}$), denoted by different colors. The total sulfate~~ . The secondary Sulfate concentration obtained from simulations without consideration of organic acid dissociation ('no diss'~~is shown as a black line~~, black line) is shown for reference. The relative changes in the ~~sulfate~~ Sulfate concentration compared to 'no diss' (~~$\Delta[SO_4^{2-}])$,~~ $\Delta[SO_4^{2-}]''$) for both oxidation pathways are given in ~~the appendix (fig. **??**).~~ fig. S3 in the Supplement.

The Sulfate concentration from H_2O_2 oxidation (panels a, b) increases drastically for both organic acids when organic acid dissociation is accounted for. From eq. 15, it may seem that ~~sulphate~~ Sulfate concentration should decrease with increasing $[H^+]_{\text{tot}}$~~concentration~~, but the reverse is observed in ~~figure **??**.~~ fig. 2. This is a property of the general acid catalysed mechanism, where the pK_a~~dependent k_{HA}~~ -dependent rate constant k_{HA} offsets the decrease in ~~sulphate concentration~~ $[SO_4^{2-}]''$ caused by increased $[H^+]_{\text{tot}}$ concentration. These results are in line with Liu et al. (2020)~~where~~ , who suggested the general acid catalysed H_2O_2 oxidation ~~was suggested as a source~~ to explain 'missing' ~~sulfate~~ Sulfate during severe haze episodes. The oxidation of SO_2 by O_3 (panels c, d) follows a straightforward dependence on $[H^+]_{\text{tot}}$ ~~concentration from~~ (eq. 16), where increased ~~hydrogen~~ Hydrogen ion concentration results in decreased $[SO_4^{2-}]''$, compared to the 'no diss' condition.

~~For malonic~~

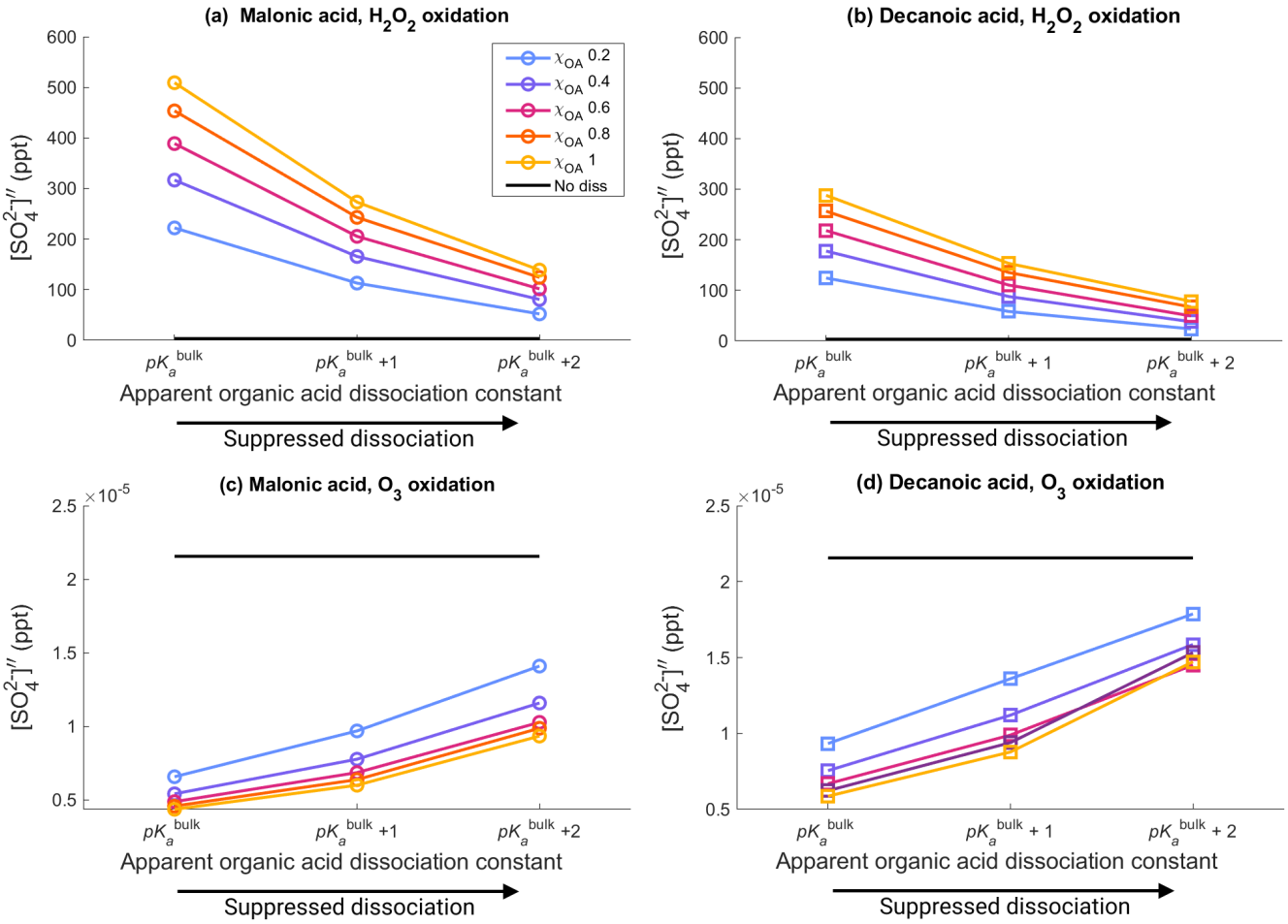

Figure 2. Aqueous aerosol secondary Sulfate concentrations $[SO_4^{2-}]''$ from oxidation of SO_2 by H_2O_2 (panels a, b, eqs. 15 and 13) and O_3 (panels c, d, eq. 16), for Malonic acid (panels a, c) and Decanoic acid (panels b, d), with varying pK_a corresponding to representations of bulk (pK_a^{bulk}) and surface modulated ($pK_a^{bulk}+1$ and 2) organic acid dissociation, in the aqueous aerosol population with sizes between $D_{wet} = 0.317 - 40$ µm, calculated in the Sulfur chemistry module of HAMBOX with five different initial organic mass fractions $\chi_{OA} = \{0.2, 0.4, 0.6, 0.8, 1\}$, denoted by blue, purple, pink, orange, and yellow, respectively (Table 2), after 1 hour of simulation time. Simulations without accounting for organic acid dissociation are represented by 'no diss' (black curves).

For Malonic acid, H_2O_2 oxidation shows an increase in ~~total sulfate~~ aqueous phase secondary Sulfate concentration compared to 'no diss' ~~, with $\Delta[SO_4^{2-}]$ ranging from 6434% to 14876%~~ (fig. 2 panel a), with $\Delta[SO_4^{2-}]''$ ranging from $6434 - 14876\%$ at pK_a^{bulk} with increasing ~~$\chi_{OA} = \{0.2, 1\}$.~~ χ_{OA} (Supplement fig. S3 panel a). With surface modulated suppressed organic ~~dissociation,~~ acid dissociation, $[SO_4^{2-}]''$ decreases compared to pK_a^{bulk}. The lowest ~~simulated $\Delta[SO_4^{2-}]$ is observed for pK_a^{bulk}+2 and χ_{OA} 0.2~~ $\Delta[SO_4^{2-}]''$ is predicted for $pK_a^{bulk}+2$ at $\chi_{OA} = 0.2$. But even ~~at this point, $\Delta[SO_4^{2-}]$ is 1432~~here, $\Delta[SO_4^{2-}]'' = 1432\%$, which is a ~~significant~~ strong increase compared to 'no diss'. Similar trends are ~~observed~~ found for the

H_2O_2 oxidation with ~~decanoic acid (sub-figure~~ Decanoic acid (fig. 2 panel b), where the highest ~~sulfate concentration~~ $[SO_4^{2-}]''$ is obtained for ~~bulk organic dissociation,~~ pK_a^{bulk} with ~~$\Delta[SO_4^{2-}]$ ranging from 3557 to 8367% corresponding to $\chi_{OA} = \{0.2, 1\}$. The lowest sulfate concentration~~ $\Delta[SO_4^{2-}]''$ ranging from $3557 - 8367\%$ with increasing χ_{OA} (Supplement fig. S3 panel b). The lowest $[SO_4^{2-}]''$ predicted for OA = ~~decanoic acid is as expected~~ Decanoic acid is seen for the stronger surface modulated suppression of organic ~~dissociation at pK_a^{bulk}+2 and χ_{OA} 0.2, with $\Delta[SO_4^{2-}]$ at this point being 598~~acid dissociation at $pK_a^{\text{bulk}} + 2$ and $\chi_{OA} = 0.2$, as expected, with $\Delta[SO_4^{2-}]'' = 598\%$. The ~~sulfate~~ aqueous phase secondary Sulfate concentration from O_3 oxidation ~~decreases by 70 to 80~~of SO_2 (fig. 2 panel c), decreases by $70 - 80\%$ compared to 'no diss' for OA = ~~malonic~~ Malonic acid at pK_a^{bulk} ~~with increasing $\chi_{OA} = \{0.2, 1\}$.~~ , with increasing χ_{OA} (Supplement fig. S3 panel c). The decrease is ~~less~~ smaller for surface modulated suppressed acid dissociation, as expected, ~~and is 35 to 55~~with $\Delta[SO_4^{2-}]'' = 35 - 55\%$ for the ~~stronger dissociation suppression at pK_a^{bulk}+2.~~ more strongly suppressed dissociation at $pK_a^{\text{bulk}} + 2$. For OA = ~~decanoic acid also shows~~ Decanoic acid (fig. 2 panel d), a similar trend ~~for sulfate concentration~~ is seen for $[SO_4^{2-}]''$ from O_3 oxidation, where decrease in ~~sulfate~~ aqueous phase secondary Sulfate concentration is in the range of ~~20 to 75~~$\Delta[SO_4^{2-}]'' = 20 - 75\%$ for bulk and surface ~~OA dissociation . Therefore, the~~ modulated suppressed dissociation (Supplement fig. S3 panel d). Therefore, H_2O_2 oxidation of SO_2 results in a far greater increase in ~~in the total~~ $[SO_4^{2-}]''$ in the aerosol population than the decrease in $[SO_4^{2-}]''$ from the O_3 oxidation of SO_2, compared to 'no diss'.

~~Thus, the increase when OA acidity and ensuing dissociation is accounted for also translates into significant increase in predicted sulfate concentration, ,~~ These results show how the increase in $[H^+]_{\text{tot}}$ from organic acid dissociation in terms of $[H^+]_{\text{HA}}$ results in significant increases in predicted $[SO_4^{2-}]''$ in the aqueous aerosol, compared to when organic acid dissociation is not accounted for. As expected, the effect is smaller when organic dissociation is suppressed ~~with~~ according to surface modulated pK_a, but even for the stronger suppression considered here, the effect is ~~1432–4000% and 598–2500% with $\chi_{OA} = \{0.2, 1\}$, for malonic acid and decanoic acid~~ $1432 - 4000\%$ and $598 - 2500\%$ with increasing χ_{OA}, for Malonic and Decanoic acid organic aerosol, respectively. We see that the effect of acid dissociation is larger for ~~the~~ H_2O_2 oxidation, suggesting that this pathway is more sensitive to inclusion of organic aerosol acidity and dissociation effects.

~~Critical supersaturation (S_i) as a function of the initial organic mass fraction (χ_{OA}) calculated using eq. 3 for (a) malonic acid and (b) decanoic acid, for three initial dry particle sizes (d_p = 135 , 290 and 456) and apparent pK_a representing bulk (pK_a^{bulk}) and surface (pK_a^{bulk}+1 and pK_a^{bulk}+2) organic dissociation. The 'no diss' represents simulation without accounting for organic dissociation.~~

3.3 Activation of droplets

Figure 3 shows the critical supersaturation S_i (eq. 3) predicted with HAMBOX for ~~the five selected~~ initial organic mass fractions ~~(χ_{OA})~~$\chi_{OA} = \{0.2, 0.4, 0.6, 0.8, 1\}$, obtained for three dry particle sizes, d_p = ~~135~~ 135 nm (darkest shade), ~~290~~ 290 nm (lighter shade) and ~~456~~ 456 nm (lightest shade), with ~~apparent~~ pK_a ~~=~~ represented by bulk (pK_a^{bulk} ~~+X, corresponding to representations of bulk (X=0, blue~~) and surface modulated (~~X=1, red and X=2, green) organic~~ $pK_a^{\text{bulk}} + 1$ and $pK_a^{\text{bulk}} + 2$) organic acid dissociation, considering ~~(a)~~ OA = ~~malonic acid , and (b)~~ Malonic acid (panel a), and OA = ~~decanoic acid. The~~ Decanoic acid (panel b). Results from simulations with the 'no diss' condition ~~is also shown~~ (black bars) are also shown in both

panels for each dry particle size~~in both figures. The aerosol size redistribution~~. The dry particle sizes chosen here fall in the Accumulation sub-range of size bins. We choose these dry particle sizes to investigate the critical supersaturation as particles in the Accumulation size range have been shown to be the most effective in CDNC production (Patel and Jiang, 2021).

The redistribution of aerosol sizes caused by the increased ~~sulfate~~ Sulfate concentrations affects the calculation of the droplet ~~radius (D_{wet}) in~~ size D_{wet} (eq. 3~~and thus, the critical supersaturation~~). Therefore, S_i is affected by bulk (pK_a^{bulk}) and surface modulated (~~pK_a^{bulk}+1 and pK_a^{bulk}+2)~~ $pK_a^{\text{bulk}}+1$ and $pK_a^{\text{bulk}}+2$) acid dissociation of the OA. We see that for both organic acids considered, the increased ~~sulfate~~ secondary Sulfate concentrations in the aqueous aerosols, compared to 'no diss', is sufficient to significantly decrease ~~the critical supersaturation for all~~ S_i for all χ_{OA} at each of the three dry particle sizes ~~and all OA mass fractions~~ considered. As expected, the decrease in S_i is ~~lesser~~ smaller when surface modulated suppressed acid dissociation is considered~~. For decanoic acid~~, compared to simulations considering bulk acidity of OA. For OA = Decanoic acid (panel b), the difference between ~~the~~ S_i calculated for bulk and surface ~~apparent (pK_a)~~ modulated pK_a is larger than ~~those calculated for malonic acid . This difference is more visible in the higher~~ for OA = Malonic acid (panel a), especially for the larger dry particle sizes (lightest shade) and higher organic mass ~~fraction (χ_{OA} 0.6 to 1)~~fractions, $\chi_{\text{OA}} = 0.6 - 1$. This suggests that ~~the simulated~~ S_i from ~~decanoic~~ consideration of Decanoic acid dissociation is more susceptible to changes in the surface ~~shifted apparent (pK_a) than malonic~~ modulated pK_a than for Malonic acid, especially at higher ~~dry particle sizes and higher organic mass fractions~~d_p and χ_{OA}. While Decanoic acid is the more surface active of the two organic acids considered, because our simple empirical representation does not explicitly account for surface adsorption, this effect is here caused by the differences in bulk and apparent surface modulated pK_a with respect to the aerosol pH. As the ~~χ_{OA}~~ organic mass fraction increases, the difference in S_i between all ~~apparent~~ pK_a conditions and 'no diss' increases for both organic acids. ~~As the~~

The calculated S_i in each ~~bin also reflects the changes in the~~ size bin also includes any changes in aerosol water activity due to ~~organic dissociation (section 2.4.4), we~~ increased organic van't Hoff factor from organic acid dissociation (eq. 34, Section 2.4.4). We see that for both organic acids, the water activity is sufficiently reduced, even for the surface modulated suppressed acid dissociation, to significantly decrease S_i, compared to 'no diss'. It is well ~~known that critical supersaturation~~ established that aerosol critical supersaturation typically increases with increasing OA ~~due to hygroscopicity (Svenningsson et al., 2006), however,~~ mass fraction, due to the higher hygroscopicity of organic aerosol components compared to other soluble species, such as inorganic salts (Svenningsson et al., 2006). However, fig. 3 shows that organic acid dissociation can partially counter this increase in S_i. This effect is smaller if surface modulated ~~suppressed organic~~ suppression of organic acid dissociation is considered, which is ~~more relevant in smaller droplets and particles due to the high surface-to-bulk ratio~~expected to be more relevant for smaller particles and droplets, due to their high surface area to bulk volume ratio, and for aerosol populations with higher fractions of surface active OA (Prisle, 2021).

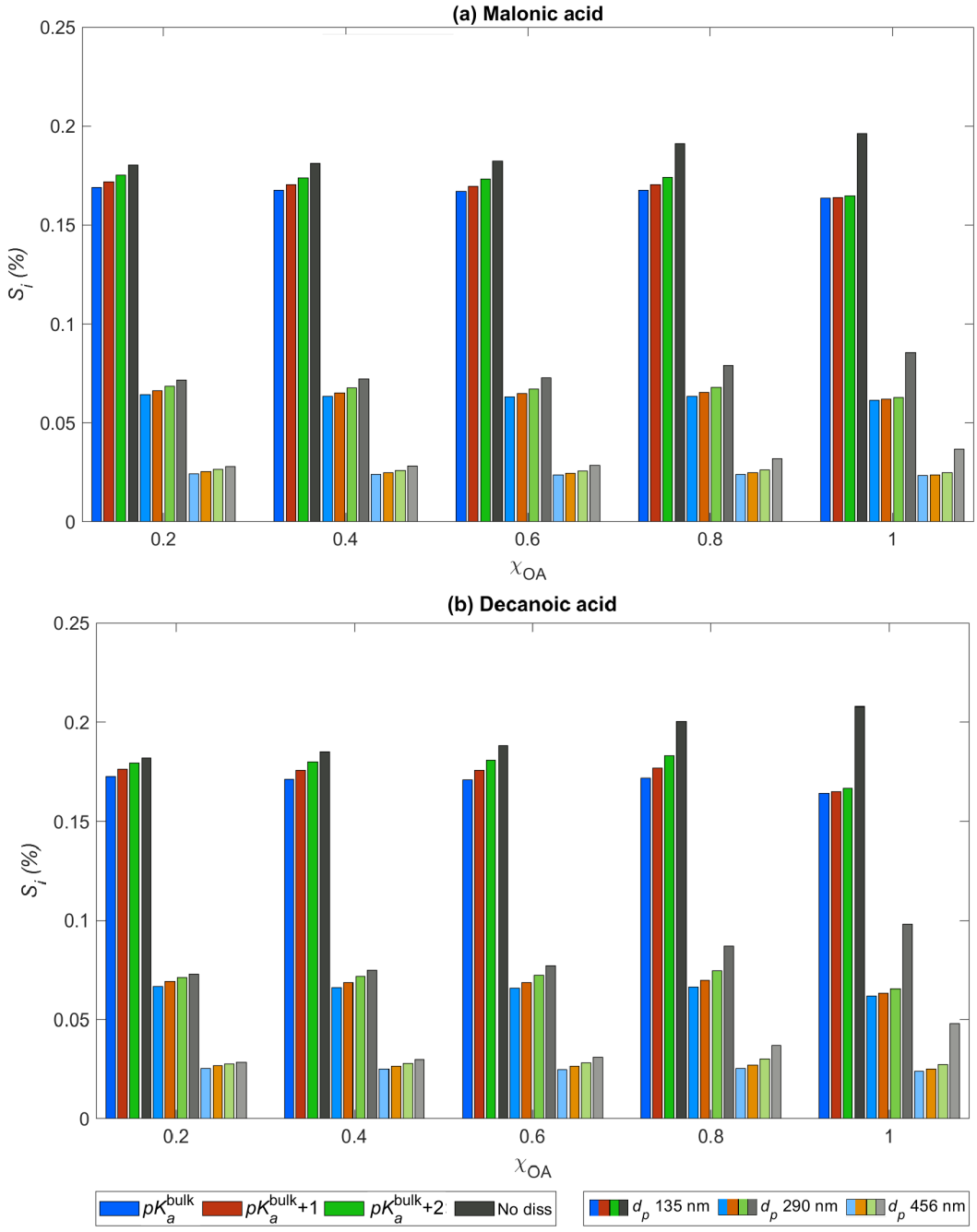

Figure 3. Critical supersaturation S_i as a function of the initial organic aerosol mass fraction χ_{OA} for (a) Malonic acid and (b) Decanoic acid, for three initial dry particle sizes, d_p = 135 nm (darkest shade), 290 nm (lighter shade), and 456 nm (lightest shade), and pK_a representing bulk (pK_a^{bulk}, in blue) and surface ($pK_a^{bulk} + 1$, in orange, and $pK_a^{bulk} + 2$, in green) organic acid dissociation. Simulations without accounting for organic acid dissociation are represented by 'no diss' (black and grey bars).

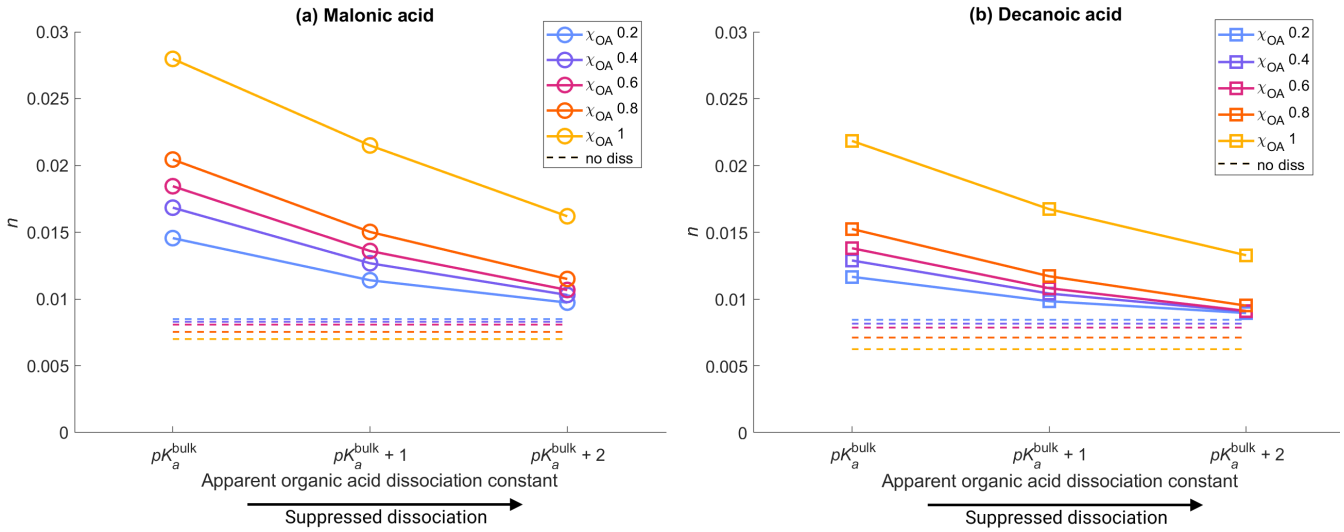

Figure 4. The average activated fraction~~(, n) in~~ , of the ~~whole~~ aerosol population with droplet ~~radius 0.317~~ sizes between $D_{wet} = 0.317 - 40$ µm~~to 40~~ , after ~~1~~ 1 hour of simulation time, ~~assuming~~ for five different initial organic mass fractions ~~(χ_{OA})~~$\chi_{OA} = \{0.2, 0.4, 0.6, 0.8, 1\}$, denoted by ~~different colors~~blue, purple, pink, orange, and yellow, respectively (see also Table 2), calculated ~~using eq. 8~~ for varying pK_a corresponding to representations of bulk (pK_a^{bulk}) and surface modulated ($pK_a^{bulk} + 1$ and 2) organic acid dissociation, and considering (a) OA = ~~malonic~~ Malonic acid, and (b) OA = ~~decanoic~~ Decanoic acid. The average activated fraction in the 'no diss' ~~average activated fraction for each χ_{OA}~~ condition is shown as ~~a~~ dashed ~~line~~ lines in corresponding colors for each χ_{OA}.

Figure 4 shows the activated fraction ~~(n)~~ (eq. 8) of the aerosol population, with droplet sizes between $D_{wet} = 0.317 - 40$ µm, averaged for all ~~size bins~~ aerosol size bins, calculated for initial organic mass fractions ~~, $\chi_{OA} = \{0.2, 1\}$, shown by different colours, calculated using eq. 8, with apparent~~ $\chi_{OA} = \{0.2, 0.4, 0.6, 0.8, 1\}$, denoted by blue, purple, pink, orange, and yellow, respectively (Table 2), with pK_a ~~=~~ representing bulk (pK_a^{bulk} ~~+X, corresponding to representations of bulk (X=0~~) and surface ~~modulated (X=1 and 2) organic~~ ($pK_a^{bulk} + 1$ and $pK_a^{bulk} + 2$) organic acid dissociation, considering ~~(a)~~ OA = ~~malonic acid , and (b)~~ Malonic acid (panel a) and OA = ~~decanoic acid. The~~ Decanoic acid (panel b). The average activated fractions for simulations not considering organic acid dissociation ('no diss' ~~average activated fraction, shown in corresponding colors~~) are shown as dashed lines ~~, approximately 0.006–0.008~~ in corresponding colors for each χ_{OA}, approximately $0.006 - 0.008$ for both organic acids~~, with $\chi_{OA} = \{0.2, 1\}$~~. The inclusion of organic ~~dissociation effects in the calculations results in a higher activated fraction~~ acid dissociation effects results in higher activated fractions than 'no diss' ~~, for both the~~ for both organic acids, with ~~malonic~~ Malonic acid dissociation resulting in a greater n than ~~decanoic aciddissociation under the same χ_{OA} and apparent~~ Decanoic acid, for the same χ_{OA} and pK_a. This is expected~~as malonic~~ , as Malonic acid is a stronger acid with lower ~~pK_a~~ pK_a^{bulk} and $[H^+]_{tot}$ from ~~malonic~~ Malonic acid dissociation under the same conditions ~~was higher than that from decanoic aciddissociation~~is higher than for Decanoic acid. The maximum activated fraction is observed for pK_a^{bulk} ~~, 0.014 to 0.027~~ with $n = 0.014 - 0.027$ for OA = ~~malonic acid and 0.012 to 0.021~~ Malonic acid and $n = 0.012 - 0.021$ for OA = ~~decanoic~~ Decanoic acid. For surface modulated suppressed organic ~~dissociation, pK_a^{bulk} +1,~~ acid dissociation according

to $pK_a^{\mathrm{bulk}}+1$, the activated fraction decreases to ~~0.011–0.021 and 0.010–0.016~~ $0.011-0.021$ and $0.010-0.016$ for OA = ~~malonic and decanoic~~ Malonic and Decanoic acids, respectively. As expected, ~~for~~ the stronger surface modulated ~~dissociation suppression, pK_a^{bulk}+2,~~ acid dissociation suppression according to $pK_a^{\mathrm{bulk}}+2$ further decreases the activated fraction~~further decreases, but~~ , but n is still higher than for 'no diss' (~~0.009–0.016 and 0.009–0.013~~ $0.009-0.016$ and $0.009-0.013$ for OA = ~~malonic and decanoic~~ Malonic and Decanoic acids, respectively~~, corresponding to $\chi_{\mathrm{OA}}=\{0.2,1\}$~~). For both organic acids, the activated fraction also increases with increasing ~~χ_{OA}~~ χ_{OA}, which is expected as the $[\mathrm{H}^+]_{\mathrm{tot}}$ increases with increasing ~~χ_{OA}~~ χ_{OA} (fig 1). For both ~~the~~ organic acids, ~~the amount of~~ $[\mathrm{H}^+]_{\mathrm{tot}}$ is ~~sufficient to decrease the critical supersaturation enough to translate~~ sufficiently high to lead to a decrease in S_i that translates into an increased activated fraction for both bulk and surface modulated suppressed organic ~~dissociation, with the effect being smaller~~ acid dissociation conditions, with a smaller effect for the suppressed acid dissociation, as expected.

3.4 Cloud droplet number concentration

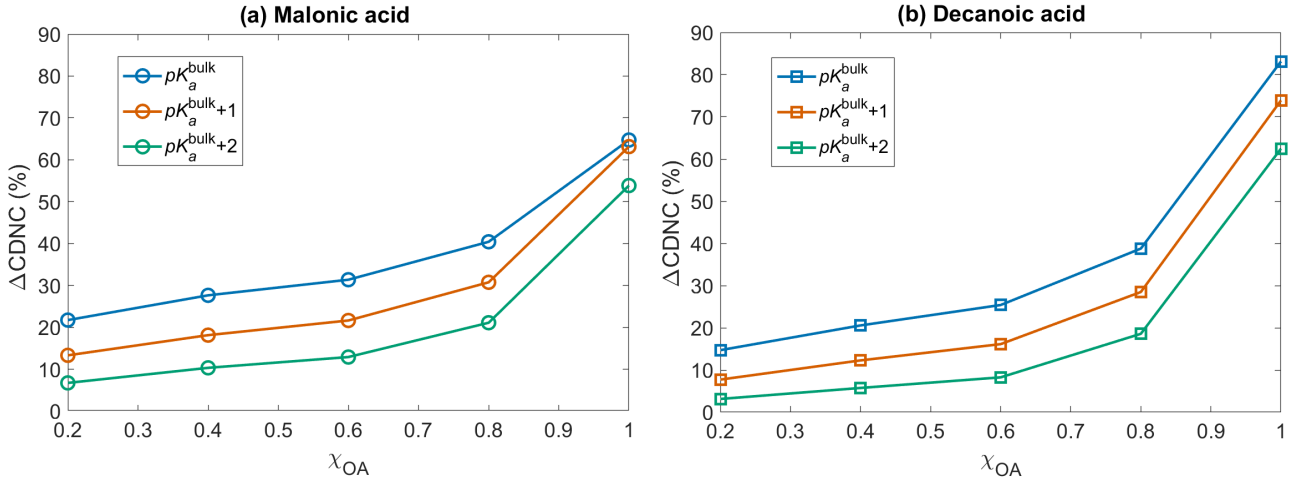

Figure 5. The change in cloud droplet number concentration ~~(~~ΔCDNC ~~, calculated using equation~~ (eq. 10) with respect to 'no diss' for (a) OA = ~~malonic~~ Malonic acid and (b) OA = ~~decanoic~~ Decanoic acid, ~~calculated using equation 10 for the five selected~~ as a function of initial organic mass fractions ~~(χ_{OA})~~ $\chi_{\mathrm{OA}}=\{0.2,0.4,0.6,0.8,1\}$ assuming organic acid dissociation ~~in the~~ according to bulk (pK_a^{bulk}, blue) and surface modulated ~~organic dissociation~~ properties (~~pK_a^{bulk}+1~~$pK_a^{\mathrm{bulk}}+1$, orange, and ~~pK_a^{bulk}+2~~$pK_a^{\mathrm{bulk}}+2$, green).

Figure 5 shows the ~~CDNC enhancement (ΔCDNC~~change in cloud droplet number concentration ΔCDNC (eq. 10) with respect to 'no diss'~~for the five selected~~ , as a function of initial organic mass ~~fraction, $\chi_{\mathrm{OA}}=\{0.2,1\}$, for (a) malonic acid and (b) decanoic acid, considering the three representations of organic dissociation with apparent~~ fractions $\chi_{\mathrm{OA}}=\{0.2,0.4,0.6,0.8,1\}$, considering OA = Malonic acid (panel a), and OA = Decanoic acid (panel b), for varying pK_a ~~at pK_a^{bulk} (~~corresponding to representations of bulk (pK_a^{bulk}, in blue), ~~pK_a^{bulk}+1 (orange) and pK_a^{bulk}+2 (green)~~ and surface modulated ($pK_a^{\mathrm{bulk}}+1$, in orange, and $pK_a^{\mathrm{bulk}}+2$, in green) organic acid dissociation. A significant enhancement in CDNC is seen for both ~~malonic~~

and decanoic acidOAMalonic and Decanoic acid, compared to when no organic acid dissociation is considered ('no diss'no diss). Similar trends are seen for both acids, where pK_a^{bulk} shows the highest CDNC enhancement compared to 'no diss'. This is expected based on the calculated $[H^+]_{\text{tot}}$ and (fig. 1) and $[SO_4^{2-}]''$ (fig. 2) from the bulk OA dissociation organic acidity and surface modulated suppressed OA organic acid dissociation and consequent critical supersaturation (S_i, fig. 3) from both organic acids. At the bulk pK_aFor pK_a^{bulk} and OA = Decanoic acid, ΔCDNC for decanoic acidranges from 14.70% to 83.14% on increasing $\chi_{\text{OA}} = \{0.2, 1\}$. For the malonic ΔCDNC ranges from 14.7% to 83.1% with increasing χ_{OA}. For OA = Malonic acid, the ΔCDNC is smallerranging from 21.73% to 64.72% for a corresponding increase in χ_{OA} at bulk apparent pK_aΔCDNC is smaller, ranging from 21.7% to 64.7% for corresponding χ_{OA} considering bulk acidity pK_a^{bulk}. Under surface modulated suppressed dissociation of pK_a^{bulk}+1organic acid dissociation $pK_a^{\text{bulk}} + 1$, the CDNC enhancement is less than that obtained from pK_a^{bulk}, ranging from 7.73% to 73.9% for decanoic acid and 13.31% to 63.15% for malonic 7.7% to 73.9% for Decanoic acid and 13.3% to 63.1% for Malonic acid. For the stronger surface modulated dissociation suppression, pK_a^{bulk}+2, the CDNC enhancement with respect to 'no diss' is 3.14% to 62.47% for decanoic acid and 6.72% to 53.85% for malonic acid, for $\chi_{\text{OA}} = \{0.2, 1\}$acid dissociation suppression $pK_a^{\text{bulk}} + 2$, ΔCDNC is 3.1% to 62.5% for OA = Decanoic acid and 6.7% to 53.9% for OA = Malonic acid, with increasing χ_{OA}.

The CDNC enhancement upon including OA acidity acid dissociation is caused by the change in aerosol size distribution due to the increased sulfate Sulfate concentrations, which shifts the size distribution towards larger particles, which are more effective in CDNC production (Hudson and Da, 1996; McFiggans et al., 2006). Since size plays a significant role in cloud-nucleating cloud droplet nucleating ability of aerosol particles (Dusek et al., 2006), the effect of organic acid dissociation on cloud response will be different depending on whether bulk or surface modulated properties are used to describe the organic aerosol, and from fig. 5 we see that this difference is significant for both malonic and decanoic Malonic and Decanoic acid under the simulation conditions. The aerosol size distribution after one hour of simulation time with and without activating the sulfur Sulfur chemistry module, for OA = malonic acid and decanoic acid considering χ_{OA} = 0.8 with apparent is given in the Supplement (figs. S4 and S5) for both organic acids, assuming initial organic mass fraction, $\chi_{\text{OA}} = 0.8$. The aerosol size distribution is shown for varying pK_a corresponding to bulk organic dissociation, surface modulated suppressed dissociation and no dissociation, is shown in the appendix (figures ?? and ??). For 'no diss'representations of bulk (pK_a^{bulk}) and surface modulated ($pK_a^{\text{bulk}} + 1$ and 2) organic acid dissociation, together with the no acid dissociation condition. Without organic acid dissociation, the size distribution is almost similar at the same after one hour for simulations with and without activating the sulfur Sulfur chemistry module, for both organic acids. For organic dissociation at bulk acidity pK_a^{bulk}, the size distribution aerosol size distribution at one hour is significantly different from the 'no diss' size distribution, at one hour. The change is smaller for the suppressed organic dissociation at pK_a^{bulk}+1 and pK_a^{bulk}+2, however the change in size distribution even from acid dissociation conditions $pK_a^{\text{bulk}} + 1$ and $pK_a^{\text{bulk}} + 2$. However, even for the stronger suppressed dissociation is significant enough to effect 6.7–53.8 % and 3.1–62.4 % ΔCDNC the change in aerosol size distribution is sufficient to yield ΔCDNC by 6.7–53.8 % and 3.1–62.4 % for OA = malonic acid and decanoic Malonic acid and Decanoic acid, respectively, compared to 'no diss'.

3.5 Short-wave radiative effect

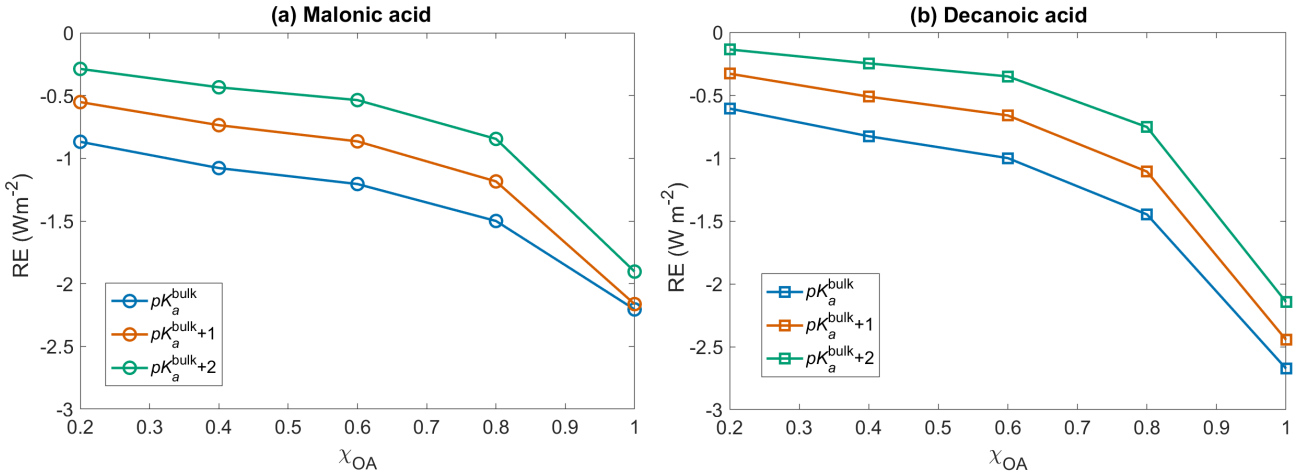

Figure 6. ~~The short~~ Short wave radiative effect (RE, ~~calculated using equation~~ eq. 12) with respect to 'no diss' for (a) ~~malonic~~ Malonic acid and (b) ~~decanoic~~ Decanoic acid, for ~~the five selected~~ varying initial organic mass fractions (χ_{OA} $\chi_{OA} = 0.2 - 1$) assuming organic dissociation ~~in the~~ according to bulk acidity (pK_a^{bulk}, blue) and surface modulated organic acid dissociation (~~$pK_a^{bulk}+1$~~ $pK_a^{bulk} + 1$, orange, and ~~$pK_a^{bulk}+2$~~ $pK_a^{bulk} + 2$, green).

Figure 6 shows the short-wave radiative effect ~~(RE~~ RE (eq. 12) with respect to 'no diss' ~~for the five selected~~, as a function of initial organic mass fractions $\chi_{OA} = 0.2 - 1$, considering OA = Malonic acid (panel a), and OA = Decanoic acid (panel b), ~~$\chi_{OA} = \{0.2, 1\}$, considering the entire organic fraction as (a) malonic acid and (b) decanoic acid, for~~ for varying pK_a corresponding to representations of bulk ~~organic dissociation, pK_a^{bulk}~~ (pK_a^{bulk}, in blue), and surface modulated ~~suppressed organic dissociation, $pK_a^{bulk}+1$ (orange) and $pK_a^{bulk}+2$(green)~~ ($pK_a^{bulk} + 1$, in orange, and $pK_a^{bulk} + 2$, in green) organic acid dissociation. The inclusion of organic acid dissociation leads to a cooling effect for both organic acids, compared to 'no diss'. Considering organic acid dissociation with bulk properties ~~with apparent pK_a at~~ (pK_a^{bulk}~~, the highest~~), a larger cooling effect is observed for both acids, ranging from ~~- 0.6 to - 2.7 for decanoic acid and - 0.86 to - 2.2 for malonic acidas χ_{OA} increases from 0.2 to 1.~~ -0.6 W m^{-2} to -2.7 W m^{-2} for Decanoic acid and -0.86 W m^{-2} to -2.2 W m^{-2} for Malonic acid, as χ_{OA} increases from 0.2 to 1. The effect is smaller when ~~considering surface modulated suppressed dissociation~~ surface modulated suppression of acid dissociation is considered, but still significant compared to 'no diss'~~, with RE ranging from -0.5 to -2.2 for malonic acid and -0.3 to -2.4 for decanoic acid at~~. For OA = Malonic acid, the range of RE extends from -0.5 W, m^{-2} to -2.2 W, m^{-2} for $pK_a^{bulk} + 1$, and from -0.3 W, m^{-2} to -1.6 W, m^{-2} for the more strongly suppressed organic acid dissociation $pK_a^{bulk} + 2$. For OA = Decanoic acid, the range of RE varies from -0.3 W, m^{-2} to -2.4 W, m^{-2} for $pK_a^{bulk} + 1$, and from -0.1 W, m^{-2} to -2.1 W, m^{-2} for $pK_a^{bulk} + 2$.

The effects of OA acid dissociation on cloud droplet number concentrations and radiative effect without considering the changes in the aqueous aerosol Sulfur chemistry are shown in fig. S6 of the Supplement. Here, the effects of organic acid

dissociation arise from modification of the van't Hoff factor i_{OA} (eq. 34), reflected as changes in the Raoult term B (eq. 4) and consequently S_i (eq. 3). The ΔCDNC and RE in fig. S6 are therefore independent of the increased $[H^+]$ driven Sulfate concentrations in the aqueous aerosol and instead reflect the change in water activity due to the dissociation of the organic acid and consequent increase in the number of available moles of solute n_s (eq. 33). Considering OA acid dissociation effects in the water activity exclusively, OA = Malonic acid shows $< 0.5\%$ ΔCDNC with respect to 'no diss' for all representations of organic acid dissociation. For OA = Decanoic acid, ΔCDNC with respect to 'no diss' is slightly higher ($\approx 1\%$), specially for bulk acidity pK_a^{bulk} ~~+1 and -0.3 to -1.6 for malonic acid and -0.1 to -2.1 for decanoic acidat pK_a^{bulk} +2.~~ and higher χ_{OA}. The resulting RE with respect to 'no diss' is within a range between 0 and -0.01 W/m^{-2} for OA = Malonic acid and 0 to -0.05 W/m^{-2} for OA = Decanoic acid.

~~Overall, our~~

3.6 Discussion

Our results show that acid dissociation of organic aerosols~~in the aqueous phase~~, exemplified with ~~common atmospheric OA~~ Malonic and Decanoic acid as common atmospheric moderately strong acids~~malonic and decanoic acid~~, can influence ~~the aqueous sulfur chemistry to have a significant effect on~~ aqueous phase Sulfur chemistry to significantly impact the cloud short-wave radiative effect. ~~A surface-modulated shifted acid-base equilibrium can change the extent to which these organic acids dissociate and therefore, the concentration of hydrogen ions at the surface is different than~~ Surface modulated suppressed acid dissociation of OA can further change the concentration of Hydrogen ions in aqueous aerosol from what is immediately expected from the bulk acidity and aerosol pH. Under these surface modulated conditions, the ~~effect of organic dissociation on the~~ effects of organic acid dissociation on cloud properties are reduced, but still significant. Since many components in atmospheric OA are ~~acidic~~both acidic and surface active, this may be important to represent in large scale models. ~~The effect of surface modulated suppressed dissociation in the atmosphere will~~ Furthermore, the impact of OA acid dissociation on cloud activating properties via aqueous phase aerosol Sulfur chemistry is significantly stronger than by changing the aerosol water activity and will be strongly underestimated if only effects on water activity are considered.

The increased Hydrogen ion concentration in aqueous aerosols as a result of OA acid dissociation leads to enhanced Sulfate mass from oxidation of SO_2 by H_2O_2. Increased Sulfate concentrations could potentially lead to enhanced formation of organosulfur compounds within the aerosols. Organosulfur compounds form in the atmosphere through heterogeneous reactions between volatile organic compounds and inorganic aerosol Sulfate and can comprise over 15% of the secondary organic aerosol mass (Brüggemann et al., 2020; Riva et al., 2019; Chen et al., 2021a; Hettiyadura et al., 2019). These organosulfur compounds could further increase OA mass and affect the resulting cloud droplet number concentrations. Organosulfates have been shown to exhibit acidic properties and primarily exist in the deprotonated form under atmospheric pH conditions (Fankhauser et al., 2022). Organosulfates are also known to be surface active in aqueous solutions (Hansen et al., 2015; Prisle et al., 2010b, . Therefore, the mechanisms of both organic acid dissociation and its surface modultation studied here for atmospheric carboxylic acids could also apply to organosulfate aerosols, potentially affecting cloud droplet activation in a similar manner.

Bulk–surface partitioning in aqueous aerosols can be seen as a form of (potentially second order) liquid-liquid phase separation (Prisle, 2023). Phase separation of organic aerosols and its impact on cloud activating properties of aerosol particles have been widely studied (Reid et al., 2018; Freedman, 2017; You et al., 2014). The partitioning of surface active aerosol components occurs between the bulk and surface phases due to differences in composition and affinity for each phase. The suppression of organic acid dissociation considered here is exactly a consequence of the increased concentration of surface active organic acid in the surface phase. Liquid-liquid phase separation in the bulk phase would effectively create two separate solutions with different compositions and ensuing properties. The modulation of organic acid dissociation could be taken into account separately for these phases, based on their individual concentrations, following analogous schemes as described by Prisle et al. (2010a) .

Our results suggest that organic acid dissociation should be considered for accurate predictions of OA chemistry and cloud microphysics in the atmosphere. The specific magnitude of predictions with the present box model implementation may not be immediately representative of analogous simulations with full 3D aerosol-chemistry-climate models, due to their greater complexity and numerous coupled processes. For example, the effect of potential surface modulated suppressed dissociation will further depend on aerosol ~~and droplet size and~~ surface activity and is expected to be especially relevant for smaller ~~aerosol sizes, and our results suggest that OA dissociation should not be omitted for accurate predictions involving organic aerosols~~droplet sizes. However, as we have used a box model version of ECHAM-HAMMOZ, implementation of the OA acid dissociation mechanisms considered here will follow analogous strategies for the full model. The box model simulations contribute insights into the detailed mechanisms of OA acid dissociation and its impact on aerosol chemistry and cloud formation and our present results provide a first assessment of the potential significance for resulting aerosol-cloud-climate parameters under conditions similar to those examined here.

4 Conclusion

We investigated the effects of organic aerosol acid dissociation on total ~~hydrogen~~ Hydrogen ion concentration in aqueous aerosols and the impact on resulting secondary ~~sulfate~~ Sulfate aerosol mass, cloud droplet number concentration, and aerosol short-wave radiative effect, using the aerosol–chemistry-climate box model ~~ECHAM6.3~~ECHAM6.3–~~HAM2.3~~HAM2.3 (HAMBOX). Simulations were carried out considering the entire OA to comprise organic acid and ~~used malonic and decanoic~~ we used Malonic and Decanoic acid as proxies for atmospheric OA ~~acids~~with different aqueous acidity and surface activity. Dissociation of organic acids was considered in three scenarios: 1) the current standard of no dissociation, 2) following ~~well-known bulk solution properties~~ well known bulk solution acidity given by the reported acid constant ~~pK_a~~pK_a^{bulk}, and 3) accounting for a surface-modulated suppression of dissociation as observed in recent laboratory experiments.

Our results show that organic ~~dissociation increases hydrogen~~ acid dissociation increases Hydrogen ion concentrations in the aqueous aerosol phase, as expected. This leads to strongly increased secondary ~~sulfate~~ Sulfate aerosol mass, which in turn decreases the critical supersaturation for cloud droplet activation and yields a higher activated ~~fraction is obtained~~ aerosol fraction than if OA acid dissociation is not considered. The cloud response is observed as enhanced cloud droplet number

concentration and a strong short-wave radiative effect of clouds. The effects of organic acid dissociation are greatest when considering the bulk acidity of OA, but still significant even when potential surface-modulated suppression of dissociation is also included.

As many atmospheric organic aerosol components are acidic (Pye et al., 2020), ~~and thereby~~ their dissociation can have significant impacts on cloud properties~~, this~~. This work highlights the importance of including ~~effects of organic dissociation~~ such organic acid dissociation effects in large scale atmospheric models. We suspect that, combined with the high surface ~~to bulk ratio and surface-bulk~~ area to bulk volume ratio and bulk–surface partitioning in small droplets (Bzdek et al., 2020; Prisle, 2021), the effects of organic dissociation and potential size dependent surface modulated acid dissociation could be significant in explaining some knowledge gaps about organic aerosol formation and acidity in atmospheric aerosols. ~~Additionally, OA~~ OA acid dissociation could be particularly relevant in explaining discrepancies of atmospheric models with observations for polluted environments (Lee et al., 2013), where organic mass fraction is usually high and the organic acid dissociation effects could become ~~more~~ very significant. Many of these organic aerosol acids may also be surface active in aqueous solutions (Gérard et al., 2019b), such as ~~activating~~ haze and activating cloud droplets, and therefore corrections to account for surface modulated suppression of organic acid dissociation may also be necessary. ~~This is expected to be particularly important for smaller size ranges, due to the high surface-to-bulk ratio of such aerosols (Bzdek et al., 2020; Prisle, 2021).~~

Code and data availability. The HAMBOX code is available from the HAMMOZ Redmine here. All simulation data and scripts underlying the figures are available here

Author contributions. GS did the model implementations and performed the calculations with contributions from MZ. GS and NLP analyzed the results and wrote the original and revised manuscripts and response to reviewers. NLP conceived, planned, supervised, and secured funding for the project. All authors approved the final text.

Competing interests. The authors declare that there is no conflict of interest.

Acknowledgements. The authors warmly thank Kunal Ghosh and Harri Kokkola for valuable support on HAMBOX. This project has received funding from the European Research Council (ERC) under the European Union's Horizon 2020 research and innovation program, project SURFACE (grant agreement no. 717022). The authors also gratefully acknowledge the financial contribution from the Academy of Finland, including grant nos. 308238, 314175, and 335649.

References

Abdul-Razzak, H.: A parameterization of aerosol activation 3. Sectional representation, Journal of Geophysical Research, 107, https://doi.org/10.1029/2001jd000483, 2002.

Abdul-Razzak, H. and Ghan, S. J.: A parameterization of aerosol activation 3. Sectional representation, Journal of Geophysical Research: Atmospheres, 107, AAC–1, 2002.

Abdul-Razzak, H., Ghan, S. J., and Rivera-Carpio, C.: A parameterization of aerosol activation: 1. Single aerosol type, Journal of Geophysical Research: Atmospheres, 103, 6123–6131, https://doi.org/10.1029/97jd03735, 1998.

Äijälä, M., Daellenbach, K. R., Canonaco, F., Heikkinen, L., Junninen, H., Petäjä, T., Kulmala, M., Prévôt, A. S., and Ehn, M.: Constructing a data-driven receptor model for organic and inorganic aerosol–a synthesis analysis of eight mass<? xmltex\break?> spectrometric data sets from a boreal forest site, Atmospheric Chemistry and Physics, 19, 3645–3672, 2019.

Andreae, M. O. and Crutzen, P. J.: Atmospheric aerosols: Biogeochemical sources and role in atmospheric chemistry, Science, 276, 1052–1058, 1997.

Angelis, M. D., Traversi, R., and Udisti, R.: Long-term trends of mono-carboxylic acids in Antarctica: Comparison of changes in sources and transport processes at the two EPICA deep drilling sites, Tellus, Series B: Chemical and Physical Meteorology, 64, 17 331, https://doi.org/10.3402/TELLUSB.V64I0.17331, 2012.

Angle, K. J., Crocker, D. R., Simpson, R. M., Mayer, K. J., Garofalo, L. A., Moore, A. N., Mora Garcia, S. L., Or, V. W., Srinivasan, S., Farhan, M., et al.: Acidity across the interface from the ocean surface to sea spray aerosol, Proceedings of the National Academy of Sciences, 118, e2018397 118, 2021.

Ault, A. P.: Aerosol Acidity: Novel measurements and implications for atmospheric chemistry, Accounts of Chemical Research, 53, 1703–1714, 2020.

Battaglia Jr, M. A., Balasus, N., Ball, K., Caicedo, V., Delgado, R., Carlton, A. G., and Hennigan, C. J.: Urban aerosol chemistry at a land–water transition site during summer–Part 2: Aerosol pH and liquid water content, Atmospheric Chemistry and Physics, 21, 18 271–18 281, 2021.

Brüggemann, M., Xu, R., Tilgner, A., Kwong, K. C., Mutzel, A., Poon, H. Y., Otto, T., Schaefer, T., Poulain, L., Chan, M. N., et al.: Organosulfates in ambient aerosol: state of knowledge and future research directions on formation, abundance, fate, and importance, Environmental Science & Technology, 54, 3767–3782, 2020.

Bzdek, B. R., Reid, J. P., Malila, J., and Prisle, N. L.: The surface tension of surfactant-containing, finite volume droplets, Proceedings of the National Academy of Sciences, 117, 8335–8343, 2020.

Chebbi, A. and Carlier, P.: Carboxylic acids in the troposphere, occurrence, sources, and sinks: A review, Atmospheric Environment, 30, 4233–4249, https://doi.org/10.1016/1352-2310(96)00102-1, 1996.

Chen, Y., Dombek, T., Hand, J., Zhang, Z., Gold, A., Ault, A. P., Levine, K. E., and Surratt, J. D.: Seasonal Contribution of Isoprene-Derived Organosulfates to Total Water-Soluble Fine Particulate Organic Sulfur in the United States, ACS Earth and Space Chemistry, 5, 2419–2432, 2021a.

Chen, Y., Guo, H., Nah, T., Tanner, D. J., Sullivan, A. P., Takeuchi, M., Gao, Z., Vasilakos, P., Russell, A. G., Baumann, K., Huey, L. G., Weber, R. J., and Ng, N. L.: Low-Molecular-Weight Carboxylic Acids in the Southeastern U.S.: Formation, Partitioning, and Implications for Organic Aerosol Aging, Environmental Science and Technology, 55, 6688–6699, https://doi.org/10.1021/ACS.EST.1C01413/ASSET/IMAGES/LARGE/ES1C01413_0006.JPEG, 2021b.

Cheng, Y., Li, S.-M., Leithead, A., Brickell, P. C., and Leaitch, W. R.: Characterizations of cis-pinonic acid and n-fatty acids on fine aerosols in the Lower Fraser Valley during Pacific 2001 Air Quality Study, Atmospheric Environment, 38, 5789–5800, 2004.

Cohn, E. J., Heyroth, F. F., and Menkin, M. F.: THE DISSOCIATION CONSTANT OF ACETIC ACID AND THE ACTIVITY COEFFICIENTS OF THE IONS IN CERTAIN ACETATE SOLUTIONS1, Journal of the American Chemical Society, 50, 696–714, 1928.

Creux, P., Lachaise, J., Graciaa, A., and Beattie, J. K.: Specific cation effects at the hydroxide-charged air/water interface, The Journal of Physical Chemistry C, 111, 3753–3755, 2007.

Drexler, C., Elias, H., Fecher, B., and Wannowius, K.: Kinetic investigation of sulfur (IV) oxidation by peroxo compounds R-OOH in aqueous solution, Fresenius' journal of analytical chemistry, 340, 605–615, 1991.

Dusek, U., Frank, G., Hildebrandt, L., Curtius, J., Schneider, J., Walter, S., Chand, D., Drewnick, F., Hings, S., Jung, D., et al.: Size matters more than chemistry for cloud-nucleating ability of aerosol particles, Science, 312, 1375–1378, 2006.

Enami, S., Hoffmann, M. R., and Colussi, A. J.: Proton availability at the air/water interface, The Journal of Physical Chemistry Letters, 1, 1599–1604, 2010.

Fankhauser, A. M., Lei, Z., Daley, K. R., Xiao, Y., Zhang, Z., Gold, A., Ault, B. S., Surratt, J. D., and Ault, A. P.: Acidity-Dependent Atmospheric Organosulfate Structures and Spectra: Exploration of Protonation State Effects via Raman and Infrared Spectroscopies Combined with Density Functional Theory, The Journal of Physical Chemistry A, 126, 5974–5984, 2022.

Feichter, J., Kjellström, E., Rodhe, H., Dentener, F., Lelieveldi, J., and Roelofs, G.-J.: Simulation of the tropospheric sulfur cycle in a global climate model, Atmospheric Environment, 30, 1693–1707, 1996a.

Feichter, J., Kjellström, E., Rodhe, H., Dentener, F., Lelieveldi, J., and Roelofs, G.-J.: Simulation of the tropospheric sulfur cycle in a global climate model, Atmospheric Environment, 30, 1693–1707, https://doi.org/https://doi.org/10.1016/1352-2310(95)00394-0, 1996b.

Franco, B., Blumenstock, T., Cho, C., Clarisse, L., Clerbaux, C., Coheur, P.-F., De Mazière, M., De Smedt, I., Dorn, H.-P., Emmerichs, T., et al.: Ubiquitous atmospheric production of organic acids mediated by cloud droplets, Nature, 593, 233–237, 2021.

Freedman, M. A.: Phase separation in organic aerosol, Chemical Society Reviews, 46, 7694–7705, 2017.

Freedman, M. A., Ott, E.-J. E., and Marak, K. E.: Role of pH in aerosol processes and measurement challenges, The Journal of Physical Chemistry A, 123, 1275–1284, 2018.

Frosch, M., Prisle, N., Bilde, M., Varga, Z., and Kiss, G.: Joint effect of organic acids and inorganic salts on cloud droplet activation, Atmospheric Chemistry and Physics, 11, 3895–3911, 2011.

Gérard, V., Noziere, B., Baduel, C., Fine, L., Frossard, A. A., and Cohen, R. C.: Anionic, cationic, and nonionic surfactants in atmospheric aerosols from the baltic coast at asko¨, sweden: Implications for cloud droplet activation, Environmental Science & Technology, 50, 2974–2982, 2016.

Gérard, V., Noziere, B., Fine, L., Ferronato, C., Singh, D. K., Frossard, A. A., Cohen, R. C., Asmi, E., Lihavainen, H., Kivekäs, N., et al.: Concentrations and adsorption isotherms for amphiphilic surfactants in PM1 aerosols from different regions of Europe, Environmental science & technology, 53, 12 379–12 388, 2019a.

Gérard, V., Noziere, B., Fine, L., Ferronato, C., Singh, D. K., Frossard, A. A., Cohen, R. C., Asmi, E., Lihavainen, H., Kiveka¨s, N., et al.: Concentrations and adsorption isotherms for amphiphilic surfactants in PM1 aerosols from different regions of Europe, Environmental science & technology, 53, 12 379–12 388, 2019b.

Goldberg, R. N., Kishore, N., and Lennen, R. M.: Thermodynamic quantities for the ionization reactions of buffers, Journal of physical and chemical reference data, 31, 231–370, 2002.

Gong, K., Ao, J., Li, K., Liu, L., Liu, Y., Xu, G., Wang, T., Cheng, H., Wang, Z., Zhang, X., et al.: Imaging of pH distribution inside individual microdroplet by stimulated Raman microscopy, Proceedings of the National Academy of Sciences, 120, e2219588 120, 2023.

Graciaa, A., Morel, G., Saulner, P., Lachaise, J., and Schechter, R.: The ζ-potential of gas bubbles, Journal of Colloid and Interface Science, 172, 131–136, 1995.

Graham, B., Guyon, P., Taylor, P. E., Artaxo, P., Maenhaut, W., Glovsky, M. M., Flagan, R. C., and Andreae, M. O.: Organic compounds present in the natural Amazonian aerosol: Characterization by gas chromatography–mass spectrometry, Journal of Geophysical Research: Atmospheres, 108, 2003.

Hallquist, M., Wenger, J. C., Baltensperger, U., Rudich, Y., Simpson, D., Claeys, M., Dommen, J., Donahue, N., George, C., Goldstein, A., et al.: The formation, properties and impact of secondary organic aerosol: current and emerging issues, Atmospheric chemistry and physics, 9, 5155–5236, 2009.

Hansen, A. M. K., Hong, J., Raatikainen, T., Kristensen, K., Ylisirniö, A., Virtanen, A., Petäjä, T., Glasius, M., and Prisle, N.: Hygroscopic properties and cloud condensation nuclei activation of limonene-derived organosulfates and their mixtures with ammonium sulfate, Atmospheric Chemistry and Physics, 15, 14 071–14 089, 2015.

Hennigan, C., Izumi, J., Sullivan, A., Weber, R., and Nenes, A.: A critical evaluation of proxy methods used to estimate the acidity of atmospheric particles, Atmospheric Chemistry and Physics, 15, 2775–2790, 2015.

Hettiyadura, A. P. S., Al-Naiema, I. M., Hughes, D. D., Fang, T., and Stone, E. A.: Organosulfates in Atlanta, Georgia: anthropogenic influences on biogenic secondary organic aerosol formation, Atmospheric Chemistry and Physics, 19, 3191–3206, 2019.

Hudson, J. G. and Da, X.: Volatility and size of cloud condensation nuclei, Journal of Geophysical Research: Atmospheres, 101, 4435–4442, 1996.

Huebert, B., Bertram, T., Kline, J., Howell, S., Eatough, D., and Blomquist, B.: Measurements of organic and elemental carbon in Asian outflow during ACE-Asia from the NSF/NCAR C-130, Journal of Geophysical Research: Atmospheres, 109, 2004.

Hung, H.-M., Hsu, M.-N., and Hoffmann, M. R.: Quantification of SO2 oxidation on interfacial surfaces of acidic micro-droplets: Implication for ambient sulfate formation, Environmental science & technology, 52, 9079–9086, 2018.

IPCC: The physical science basis, Contribution of working group I to the fifth assessment report of the intergovernmental panel on climate change, 1535, 2013, 2013.

IPCC, C. C. et al.: The physical science basis. Contribution of working group I to the fourth assessment report of the Intergovernmental Panel on Climate Change, Cambridge University Press, Cambridge, United Kingdom and New York, NY, USA, 996, 113–119, 2007.

Jacob, D. J.: Chemistry of OH in remote clouds and its role in the production of formic acid and peroxymonosulfate, Journal of Geophysical Research: Atmospheres, 91, 9807–9826, https://doi.org/10.1029/JD091ID09P09807, 1986.

Jacobson, M. Z.: Fundamentals of Atmospheric Modeling, Cambridge University Press, Cambridge, 2 edn., https://doi.org/DOI: 10.1017/CBO9781139165389, 2005.

Kanakidou, M., Seinfeld, J., Pandis, S., Barnes, I., Dentener, F. J., Facchini, M. C., Van Dingenen, R., Ervens, B., Nenes, A., Nielsen, C., et al.: Organic aerosol and global climate modelling: a review, Atmospheric Chemistry and Physics, 5, 1053–1123, 2005.

Karraker, K. and Radke, C.: Disjoining pressures, zeta potentials and surface tensions of aqueous non-ionic surfactant/electrolyte solutions: theory and comparison to experiment, Advances in colloid and interface science, 96, 231–264, 2002.

Kawamura, K., Ng, L. L., and Kaplan, I. R.: Determination of Organic Acids (C1-C10) in the Atmosphere, Motor Exhausts, and Engine Oils, Environmental Science and Technology, 19, 1082–1086, https://doi.org/10.1021/ES00141A010/ASSET/ES00141A010.FP.PNG_V03, 1985.

Keene, W. C. and Galloway, J. N.: Organic acidity in precipitation of North America, Atmospheric Environment (1967), 18, 2491–2497, https://doi.org/10.1016/0004-6981(84)90020-9, 1984.

Kokkola, H., Kühn, T., Laakso, A., Bergman, T., Lehtinen, K. E., Mielonen, T., Arola, A., Stadtler, S., Korhonen, H., Ferrachat, S., et al.: SALSA2. 0: The sectional aerosol module of the aerosol–chemistry–climate model ECHAM6. 3.0-HAM2. 3-MOZ1. 0, Geoscientific model development, 11, 3833–3863, 2018.

Kroflič, A., Frka, S., Simmel, M., Wex, H., and Grgić, I.: Size-Resolved Surface-Active Substances of Atmospheric Aerosol: Reconsideration of the Impact on Cloud Droplet Formation, Environmental Science & Technology, 52, 9179–9187, https://doi.org/10.1021/acs.est.8b02381, 2018.

Lee, L., Pringle, K., Reddington, C., Mann, G., Stier, P., Spracklen, D., Pierce, J., and Carslaw, K.: The magnitude and causes of uncertainty in global model simulations of cloud condensation nuclei, Atmospheric Chemistry and Physics, 13, 8879–8914, 2013.

Legg, S.: IPCC, 2021: Climate change 2021-the physical science basis, Interaction, 49, 44–45, 2021.

Li, J., Zhu, C., Chen, H., Fu, H., Xiao, H., Wang, X., Herrmann, H., and Chen, J.: A more important role for the ozone-S (IV) oxidation pathway due to decreasing acidity in clouds, Journal of Geophysical Research: Atmospheres, 125, e2020JD033 220, 2020.

Li, M., Su, H., Zheng, G., Kuhn, U., Kim, N., Li, G., Ma, N., Po¨schl, U., and Cheng, Y.: Aerosol pH and Ion Activities of HSO4–and SO42–in Supersaturated Single Droplets, Environmental Science & Technology, 56, 12 863–12 872, 2022.

Li, Y.-c. and Yu, J. Z.: Simultaneous determination of mono-and dicarboxylic acids, ω-oxo-carboxylic acids, midchain ketocarboxylic acids, and aldehydes in atmospheric aerosol samples, Environmental science & technology, 39, 7616–7624, 2005.

Lin, J. J., Malila, J., and Prisle, N. L.: Cloud droplet activation of organic–salt mixtures predicted from two model treatments of the droplet surface, Environmental Science: Processes & Impacts, 20, 1611–1629, 2018.

Lin, J. J., Kristensen, T. B., Calderón, S. M., Malila, J., and Prisle, N. L.: Effects of surface tension time-evolution for CCN activation of a complex organic surfactant, Environmental Science: Processes & Impacts, 22, 271–284, 2020.

Liu, T., Clegg, S. L., and Abbatt, J. P.: Fast oxidation of sulfur dioxide by hydrogen peroxide in deliquesced aerosol particles, Proceedings of the National Academy of Sciences, 117, 1354–1359, 2020.

Liu, Y., Wu, Z., Huang, X., Shen, H., Bai, Y., Qiao, K., Meng, X., Hu, W., Tang, M., and He, L.: Aerosol phase state and its link to chemical composition and liquid water content in a subtropical coastal megacity, Environmental science & technology, 53, 5027–5033, 2019.

Lohmann, U. and Lesins, G.: Stronger constraints on the anthropogenic indirect aerosol effect, Science, 298, 1012–1015, 2002.

Maaß, F., Elias, H., and Wannowius, K. J.: Kinetics of the oxidation of hydrogen sulfite by hydrogen peroxide in aqueous solution:: ionic strength effects and temperature dependence, Atmospheric Environment, 33, 4413–4419, 1999.

Malila, J. and Prisle, N.: A monolayer partitioning scheme for droplets of surfactant solutions, Journal of advances in modeling earth systems, 10, 3233–3251, 2018.

Margarella, A. M., Perrine, K. A., Lewis, T., Faubel, M., Winter, B., and Hemminger, J. C.: Dissociation of sulfuric acid in aqueous solution: determination of the photoelectron spectral fingerprints of H2SO4, HSO4–, and SO42–in water, The Journal of Physical Chemistry C, 117, 8131–8137, 2013.

Martell, A. E. and Smith, R. M.: Critical stability constants, vol. 1, Springer, 1974.

Masson-Delmotte, V., Zhai, P., Pirani, A., Connors, S. L., Péan, C., Berger, S., Caud, N., Chen, Y., Goldfarb, L., Gomis, M., et al.: Climate change 2021: the physical science basis, Contribution of working group I to the sixth assessment report of the intergovernmental panel on climate change, 2, 2021.

McArdle, J. V. and Hoffmann, M. R.: Kinetics and mechanism of the oxidation of aquated sulfur dioxide by hydrogen peroxide at low pH, The Journal of Physical Chemistry, 87, 5425–5429, 1983.

McFiggans, G., Artaxo, P., Baltensperger, U., Coe, H., Facchini, M. C., Feingold, G., Fuzzi, S., Gysel, M., Laaksonen, A., Lohmann, U., et al.: The effect of physical and chemical aerosol properties on warm cloud droplet activation, Atmospheric Chemistry and Physics, 6, 2593–2649, 2006.

Michailoudi, G., Hyttinen, N., Kurten, T., and Prisle, N. L.: Solubility and Activity Coefficients of Atmospheric Surfactants in Aqueous Solution Evaluated Using COSMO therm, The Journal of Physical Chemistry A, 124, 430–443, 2019.

Millet, D. B., Baasandorj, M., Farmer, D. K., Thornton, J. A., Baumann, K., Brophy, P., Chaliyakunnel, S., Gouw, J. A. D., Graus, M., Hu, L., Koss, A., Lee, B. H., Lopez-Hilfiker, F. D., Neuman, J. A., Paulot, F., Peischl, J., Pollack, I. B., Ryerson, T. B., Warneke, C., Williams, B. J., and Xu, J.: A large and ubiquitous source of atmospheric formic acid, Atmospheric Chemistry and Physics, 15, 6283–6304, https://doi.org/10.5194/ACP-15-6283-2015, 2015.

Mochida, M., Kawabata, A., Kawamura, K., Hatsushika, H., and Yamazaki, K.: Seasonal variation and origins of dicarboxylic acids in the marine atmosphere over the western North Pacific, Journal of Geophysical Research: Atmospheres, 108, 2003.

Mochizuki, T., Kawamura, K., Aoki, K., and Sugimoto, N.: Long-range atmospheric transport of volatile monocarboxylic acids with Asian dust over a high mountain snow site, central Japan, Atmospheric Chemistry and Physics, 16, 14 621–14 633, https://doi.org/10.5194/ACP-16-14621-2016, 2016.

Murphy, D., Cziczo, D., Froyd, K., Hudson, P., Matthew, B., Middlebrook, A., Peltier, R., Sullivan, A., Thomson, D., and Weber, R.: Single-particle mass spectrometry of tropospheric aerosol particles, Journal of Geophysical Research: Atmospheres, 111, 2006.

Narukawa, M., Kawamura, K., Li, S.-M., and Bottenheim, J.: Dicarboxylic acids in the Arctic aerosols and snowpacks collected during ALERT 2000, Atmospheric Environment, 36, 2491–2499, 2002.

Noziere, B., Baduel, C., and Jaffrezo, J.-L.: The dynamic surface tension of atmospheric aerosol surfactants reveals new aspects of cloud activation, Nature communications, 5, 3335, 2014.

Nozière, B., Gérard, V., Baduel, C., and Ferronato, C.: Extraction and characterization of surfactants from atmospheric aerosols, JoVE (Journal of Visualized Experiments), p. e55622, 2017.

O'Dowd, C. D., Facchini, M. C., Cavalli, F., Ceburnis, D., Mircea, M., Decesari, S., Fuzzi, S., Yoon, Y. J., and Putaud, J.-P.: Biogenically driven organic contribution to marine aerosol, Nature, 431, 676–680, 2004.

Öhrwall, G., Prisle, N. L., Ottosson, N., Werner, J., Ekholm, V., Walz, M.-M., and Bjo¨rneholm, O.: Acid–base speciation of carboxylate ions in the surface region of aqueous solutions in the presence of ammonium and aminium ions, The Journal of Physical Chemistry B, 119, 4033–4040, 2015a.

Öhrwall, G., Prisle, N. L., Ottosson, N., Werner, J., Ekholm, V., Walz, M.-M., and Bjo¨rneholm, O.: Acid–base speciation of carboxylate ions in the surface region of aqueous solutions in the presence of ammonium and aminium ions, The Journal of Physical Chemistry B, 119, 4033–4040, 2015b.

Patel, P. N. and Jiang, J. H.: Cloud condensation nuclei characteristics at the Southern Great Plains site: role of particle size distribution and aerosol hygroscopicity, Environmental Research Communications, 3, 075 002, 2021.

Peng, X., Vasilakos, P., Nenes, A., Shi, G., Qian, Y., Shi, X., Xiao, Z., Chen, K., Feng, Y., and Russell, A. G.: Detailed analysis of estimated pH, activity coefficients, and ion concentrations between the three aerosol thermodynamic models, Environmental Science & Technology, 53, 8903–8913, 2019.

Petersen, P. B. and Saykally, R. J.: Evidence for an enhanced hydronium concentration at the liquid water surface, The Journal of Physical Chemistry B, 109, 7976–7980, 2005.

Petersen, P. B. and Saykally, R. J.: Is the liquid water surface basic or acidic? Macroscopic vs. molecular-scale investigations, Chemical Physics Letters, 458, 255–261, 2008.

Petters, S. S. and Petters, M. D.: Surfactant effect on cloud condensation nuclei for two-component internally mixed aerosols, Journal of Geophysical Research: Atmospheres, 121, 1878–1895, 2016.

Prisle, N.: Cloud Condensation Nuclei Properties of Organic Aerosol Particles: Effects of Acid Dissociation and Surfactant Partitioning, University of Copenhagen, 52, 2006.

Prisle, N., Dal Maso, M., and Kokkola, H.: A simple representation of surface active organic aerosol in cloud droplet formation, Atmospheric Chemistry and Physics, 11, 4073–4083, 2011.

Prisle, N. L.: A predictive thermodynamic framework of cloud droplet activation for chemically unresolved aerosol mixtures, including surface tension, non-ideality, and bulk–surface partitioning, Atmospheric Chemistry and Physics, 21, 16 387–16 411, 2021.

Prisle, N. L.: Surfaces of Atmospheric Droplet Models Probed with Synchrotron XPS on a Liquid Microjet, Accounts of Chemical Research, https://doi.org/10.1021/acs.accounts.3c00201, 2023.

Prisle, N. L., Raatikainen, T., Sorjamaa, R., Svenningsson, B., Laaksonen, A., and Bilde, M.: Surfactant partitioning in cloud droplet activation: a study of C8, C10, C12 and C14 normal fatty acid sodium salts, Tellus B: Chemical and Physical Meteorology, 60, 416–431, 2008.

Prisle, N. L., Engelhart, G., Bilde, M., and Donahue, N.: Humidity influence on gas-particle phase partitioning of α-pinene+ O3 secondary organic aerosol, Geophysical Research Letters, 37, 2010a.

Prisle, N. L., Raatikainen, T., Laaksonen, A., and Bilde, M.: Surfactants in cloud droplet activation: mixed organic-inorganic particles, Atmospheric Chemistry and Physics, 10, 5663–5683, 2010b.

Prisle, N. L., Asmi, A., Topping, D., Partanen, A. I., Romakkaniemi, S., Dal Maso, M., Kulmala, M., Laaksonen, A., Lehtinen, K. E. J., McFiggans, G., and Kokkola, H.: Surfactant effects in global simulations of cloud droplet activation, Geophysical Research Letters, 39, L05 802, https://doi.org/10.1029/2003JD004485, 2012a.

Prisle, N. L., Ottosson, N., Öhrwall, G., Söderström, J., Dal Maso, M., and Björneholm, O.: Surface/bulk partitioning and acid/base speciation of aqueous decanoate: direct observations and atmospheric implications, Atmospheric Chemistry and Physics, 12, 12 227–12 242, https://doi.org/10.5194/acp-12-12227-2012, 2012b.

Putaud, J.-P., Raes, F., Van Dingenen, R., Brüggemann, E., Facchini, M.-C., Decesari, S., Fuzzi, S., Gehrig, R., Hüglin, C., Laj, P., et al.: A European aerosol phenomenology—2: chemical characteristics of particulate matter at kerbside, urban, rural and background sites in Europe, Atmospheric environment, 38, 2579–2595, 2004.

Putaud, J.-P., Van Dingenen, R., Alastuey, A., Bauer, H., Birmili, W., Cyrys, J., Flentje, H., Fuzzi, S., Gehrig, R., Hansson, H.-C., et al.: A European aerosol phenomenology–3: Physical and chemical characteristics of particulate matter from 60 rural, urban, and kerbside sites across Europe, Atmospheric Environment, 44, 1308–1320, 2010.

Pye, H. O., Nenes, A., Alexander, B., Ault, A. P., Barth, M. C., Clegg, S. L., Collett Jr, J. L., Fahey, K. M., Hennigan, C. J., Herrmann, H., et al.: The acidity of atmospheric particles and clouds, Atmospheric chemistry and physics, 20, 4809–4888, 2020.

Reid, J. P., Bertram, A. K., Topping, D. O., Laskin, A., Martin, S. T., Petters, M. D., Pope, F. D., and Rovelli, G.: The viscosity of atmospherically relevant organic particles, Nature communications, 9, 956, 2018.

Riva, M., Chen, Y., Zhang, Y., Lei, Z., Olson, N. E., Boyer, H. C., Narayan, S., Yee, L. D., Green, H. S., Cui, T., et al.: Increasing isoprene epoxydiol-to-inorganic sulfate aerosol ratio results in extensive conversion of inorganic sulfate to organosulfur forms: implications for aerosol physicochemical properties, Environmental science & technology, 53, 8682–8694, 2019.

Roberts, G. C., Andreae, M. O., Zhou, J., and Artaxo, P.: Cloud condensation nuclei in the Amazon Basin:"Marine" conditions over a continent?, Geophysical research letters, 28, 2807–2810, 2001.

Ruan, X., Zhao, C., Zaveri, R. A., He, P., Wang, X., Shao, J., and Geng, L.: Simulations of aerosol pH in China using WRF-Chem (v4. 0): sensitivities of aerosol pH and its temporal variations during haze episodes, Geoscientific Model Development, 15, 6143–6164, 2022.

Saxena, P. and Hildemann, L. M.: Water-soluble organics in atmospheric particles: A critical review of the literature and application of thermodynamics to identify candidate compounds, Journal of atmospheric chemistry, 24, 57–109, 1996.

Saykally, R. J.: Two sides of the acid–base story, Nature chemistry, 5, 82–84, 2013.

Seinfeld, J. H., Bretherton, C., Carslaw, K. S., Coe, H., DeMott, P. J., Dunlea, E. J., Feingold, G., Ghan, S., Guenther, A. B., Kahn, R., et al.: Improving our fundamental understanding of the role of aerosol- cloud interactions in the climate system, Proceedings of the National Academy of Sciences, 113, 5781–5790, 2016.

Stahl, P. H. and Wermuth, C. G.: Handbook of pharmaceutical salts: properties, selection and use, Chem. Int, 24, 21, 2002.

Stocker, T. F., Qin, D., Plattner, G.-K., Tignor, M. M., Allen, S. K., Boschung, J., Nauels, A., Xia, Y., Bex, V., and Midgley, P. M.: Climate Change 2013: The physical science basis. contribution of working group I to the fifth assessment report of IPCC the intergovernmental panel on climate change, 2014.

Svenningsson, B., Rissler, J., Swietlicki, E., Mircea, M., Bilde, M., Facchini, M., Decesari, S., Fuzzi, S., Zhou, J., Mønster, J., et al.: Hygroscopic growth and critical supersaturations for mixed aerosol particles of inorganic and organic compounds of atmospheric relevance, Atmospheric Chemistry and Physics, 6, 1937–1952, 2006.

Takahashi, M.: ζ potential of microbubbles in aqueous solutions: electrical properties of the gas- water interface, The Journal of Physical Chemistry B, 109, 21 858–21 864, 2005.

Tedetti, M., Kawamura, K., Charrière, B., Chevalier, N., and Sempéré, R.: Determination of low molecular weight dicarboxylic and ketocarboxylic acids in seawater samples, Analytical chemistry, 78, 6012–6018, 2006.

Tegen, I., Neubauer, D., Ferrachat, S., Siegenthaler-Le Drian, C., Bey, I., Schutgens, N., Stier, P., Watson-Parris, D., Stanelle, T., Schmidt, H., et al.: The global aerosol–climate model ECHAM6. 3–HAM2. 3–Part 1: Aerosol evaluation, Geoscientific Model Development, 12, 1643–1677, 2019.

Thompson, A.: Simulating the adiabatic ascent of atmospheric air parcels using the cloud chamber, Department of Meteorology, Penn State, pp. 121–123, 2007.

Tilgner, A., Bräuer, P., Wolke, R., and Herrmann, H.: Modelling multiphase chemistry in deliquescent aerosols and clouds using CAPRAM3. 0i, Journal of Atmospheric Chemistry, 70, 221–256, 2013.

Tilgner, A., Schaefer, T., Alexander, B., Barth, M., Collett Jr, J. L., Fahey, K. M., Nenes, A., Pye, H. O., Herrmann, H., and McNeill, V. F.: Acidity and the multiphase chemistry of atmospheric aqueous particles and clouds, Atmospheric Chemistry and Physics, 21, 13 483–13 536, 2021a.

Tilgner, A., Schaefer, T., Alexander, B., Barth, M., Collett Jr, J. L., Fahey, K. M., Nenes, A., Pye, H. O. T., Herrmann, H., and McNeill, V. F.: Acidity and the multiphase chemistry of atmospheric aqueous particles and clouds, Atmospheric Chemistry and Physics, 21, 13 483–13 536, https://doi.org/10.5194/acp-21-13483-2021, 2021b.

Tunved, P., Nilsson, E., Hansson, H.-C., Ström, J., Kulmala, M., Aalto, P., and Viisanen, Y.: Aerosol characteristics of air masses in northern Europe: Influences of location, transport, sinks, and sources, Journal of Geophysical Research: Atmospheres, 110, 2005.

Tunved, P., Stroöm, J., Kulmala, M., Kerminen, V.-M., Dal Maso, M., Svenningson, B., Lunder, C., and Hansson, H.-C.: The natural aerosol over Northern Europe and its relation to anthropogenic emissions—implications of important climate feedbacks, Tellus B: Chemical and Physical Meteorology, 60, 473–484, 2008.

Turnock, S., Mann, G., Woodhouse, M., Dalvi, M., O'Connor, F., Carslaw, K., and Spracklen, D.: The impact of changes in cloud water pH on aerosol radiative forcing, Geophysical Research Letters, 46, 4039–4048, 2019.

Twomey, S.: The influence of pollution on the shortwave albedo of clouds, Journal of the atmospheric sciences, 34, 1149–1152, 1977.

Vepsäläinen, S., Calderón, S. M., Malila, J., and Prisle, N. L.: Comparison of six approaches to predicting droplet activation of surface active aerosol–Part 1: moderately surface active organics, Atmospheric Chemistry and Physics, 22, 2669–2687, 2022.

Vepsäläinen, S., Calderón, S. M., and Prisle, N. L.: Comparison of six approaches to predicting droplet activation of surface active aerosol–Part 2: strong surfactants, EGUsphere, pp. 1–23, 2023.

Wang, G., Zhang, F., Peng, J., Duan, L., Ji, Y., Marrero-Ortiz, W., Wang, J., Li, J., Wu, C., Cao, C., et al.: Particle acidity and sulfate production during severe haze events in China cannot be reliably inferred by assuming a mixture of inorganic salts, Atmospheric Chemistry and Physics, 18, 10 123–10 132, 2018.

Wellen, B. A., Lach, E. A., and Allen, H. C.: Surface p K a of octanoic, nonanoic, and decanoic fatty acids at the air–water interface: Applications to atmospheric aerosol chemistry, Physical Chemistry Chemical Physics, 19, 26 551–26 558, 2017.

Werner, J., Julin, J., Dalirian, M., Prisle, N. L., Öhrwall, G., Persson, I., Björneholm, O., and Riipinen, I.: Succinic acid in aqueous solution: connecting microscopic surface composition and macroscopic surface tension, Physical Chemistry Chemical Physics, 16, 21 486–21 495, 2014a.

Werner, J., Julin, J., Dalirian, M., Prisle, N. L., Öhrwall, G., Persson, I., Björneholm, O., and Riipinen, I.: Succinic acid in aqueous solution: connecting microscopic surface composition and macroscopic surface tension, Phys. Chem. Chem. Phys., https://doi.org/10.1039/C4CP02776K, 2014b.

Werner, J., Persson, I., Björneholm, O., Kawecki, D., Saak, C.-M., Walz, M.-M., Ekholm, V., Unger, I., Valtl, C., Caleman, C., et al.: Shifted equilibria of organic acids and bases in the aqueous surface region, Physical Chemistry Chemical Physics, 20, 23 281–23 293, 2018.

Wu, L., Wei, L., Wang, G., and Zhao, J.: Comparison of Atmospheric Monocarboxylic and Dicarboxylic Acids in Xi' an, China, for Source Apportionment of Organic Aerosols, Water, Air, and Soil Pollution, 231, 1–11, https://doi.org/10.1007/S11270-020-04675-Y/FIGURES/5, 2020.

Yassaa, N., Meklati, B. Y., Cecinato, A., and Marino, F.: Particulate n-alkanes, n-alkanoic acids and polycyclic aromatic hydrocarbons in the atmosphere of Algiers City Area, Atmospheric Environment, 35, 1843–1851, 2001.

Yli-Juuti, T., Barsanti, K., Hildebrandt Ruiz, L., Kieloaho, A.-J., Makkonen, U., Petäjä, T., Ruuskanen, T., Kulmala, M., and Riipinen, I.: Model for acid-base chemistry in nanoparticle growth (MABNAG), Atmospheric Chemistry and Physics, 13, 12 507–12 524, 2013.

You, Y., Smith, M. L., Song, M., Martin, S. T., and Bertram, A. K.: Liquid–liquid phase separation in atmospherically relevant particles consisting of organic species and inorganic salts, International Reviews in Physical Chemistry, 33, 43–77, 2014.